Nano-Micro Letters
e-ISSN 2150-5551
CN 31-2103/TB
REVIEW
https://doi.org/10.1007/s40820-024-01418-0

Cite as
Nano-Micro Lett.
(2024) 16:215

Received: 19 February 2024
Accepted: 11 April 2024

M_4X_3 MXenes: Application in Energy Storage Devices

Iftikhar Hussain[1] ✉, Waqas Ul Arifeen[2], Shahid Ali Khan[1], Sikandar Aftab[3], Muhammad Sufyan Javed[4], Sajjad Hussain[5], Muhammad Ahmad[1], Xi Chen[1], Jiyun Zhao[1], P. Rosaiah[6], Khaled Fahmi Fawy[7], Adnan Younis[8] ✉, Sumanta Sahoo[9] ✉, Kaili Zhang[1] ✉

HIGHLIGHTS

- A systematic overview of the latest advancements in M_4X_3 MXenes is dicussed.
- The detailed properties of MXene are summarized.
- M_4X_3 MXenes are explored as an electrode material.

ABSTRACT MXene has garnered widespread recognition in the scientific community due to its remarkable properties, including excellent thermal stability, high conductivity, good hydrophilicity and dispersibility, easy processability, tunable surface properties, and admirable flexibility. MXenes have been categorized into different families based on the number of M and X layers in $M_{n+1}X_n$, such as M_2X, M_3X_2, M_4X_3, and, recently, M_5X_4. Among these families, M_2X and M_3X_2, particularly Ti_3C_2, have been greatly explored while limited studies have been given to M_5X_4 MXene synthesis. Meanwhile, studies on the M_4X_3 MXene family have developed recently, hence, demanding a compilation of evaluated studies. Herein, this review provides a systematic overview of the latest advancements in M_4X_3 MXenes, focusing on their properties and applications in energy storage devices. The objective of this review is to provide guidance to researchers on fostering M_4X_3 MXene-based nanomaterials, not only for energy storage devices but also for broader applications.

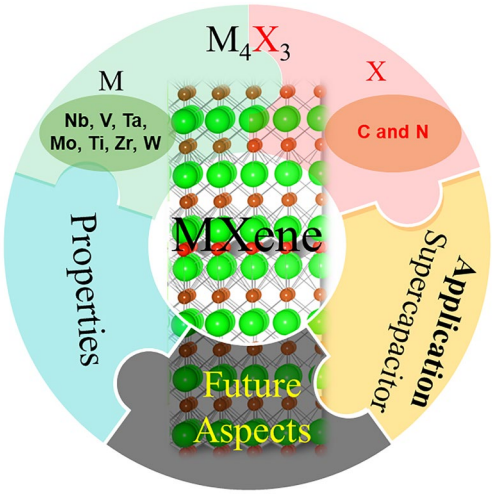

KEYWORDS MXene; M_4X_3 MXenes; 2D materials; Energy storage; Properties

Iftikhar Hussain and Waqas Ul Arifeen contributed equally to this work.

✉ Iftikhar Hussain, ihussaintoori1@gmail.com; Adnan Younis, adnaanyounis@yahoo.com; Sumanta Sahoo, sumanta95@gmail.com; Kaili Zhang, kaizhang@cityu.edu.hk

[1] Department of Mechanical Engineering, City University of Hong Kong, 83 Tat Chee Avenue, Kowloon Tong, Hong Kong, People's Republic of China
[2] School of Mechanical Engineering, Yeungnam University, Daehak-ro, Gyeongsan-si, Gyeongbuk-do 38541, South Korea
[3] Department of Semiconductor Systems Engineering and Clean Energy, Sejong University, Seoul 05006, Republic of Korea
[4] School of Physical Science and Technology, Lanzhou University, Lanzhou 730000, People's Republic of China
[5] Department of Nanotechnology and Advanced Materials Engineering, Sejong University, Seoul 05006, Republic of Korea
[6] Department of Physics, Saveetha School of Engineering, Saveetha Institute of Medical and Technical Sciences (SIMATS), Thandalam, Chennai 602 105, India
[7] Department of Chemistry, Faculty of Science, King Khalid University, P.O. Box 9004, 61413 Abha, Saudi Arabia
[8] Department of Physics, College of Science, United Arab Emirates University, P.O. Box 15551, Al-Ain, United Arab Emirates
[9] School of Chemical Engineering, Yeungnam University, Gyeongsan, Gyeongbuk 38541, South Korea

Published online: 14 June 2024

1 Introduction

Two-dimensional (2D) materials offer superior electronic structures, high specific surface areas, and other properties compared to their bulk counterparts [1, 2]. Graphene has been extensively studied as a prominent 2D material. There is a growing interest in exploring other 2D materials such as metal oxides and hydroxides, metal dichalcogenides, and hexagonal boron nitride [3–7]. Each 2D materials have been studied in various applications due to their unique properties [4, 8]. These 2D material properties make them suitable for a variety of applications, including; solar cells and touch screens [9], transistors [10], lasers [11], and biosensors [12] compared to the bulk counterparts of these 2D materials. By increasing complexity and diversity, it becomes possible to achieve exceptional combinations of properties. Further, 2D materials present convenient nanoscale building blocks for assembling architectures. In 2011, a significant addition to the family of 2D materials was made with the discovery of MXenes [13]. MXenes encompass an extensive array of two-dimensional (2D) materials, consisting of transition-metal carbides, nitrides, and carbonitrides [14–17].

Among various 2D materials, MXenes represent a diverse family of 2D materials encompassing an infinite number of solid-solution MXenes, numerous compositions predicted through computational methods, and over 50 stoichiometric MXenes that have been successfully synthesized [18]. MXenes exhibit a unique combination of optical, electronic, mechanical, and colloidal properties, making them highly versatile materials [19–22]. To be specific, this class of materials display superior conductivity, enhanced surface area, improved electrochemical performance, improved hydrophilicity, and better chemical stability than majority of its conventional 2D counterparts [23–25]. By etching the A element from MAX (M is an early transition metal; A is an element from group 13 or 14 of the periodic table, commonly Al or Si precursor phase, 2D layers are produced called MXene [26–29]. The general formula for the MXene is $M_{n+1}X_nT_x$, where M is a transition metal, X is C or N, n = 1–4, and T_x is the surface termination. The typical solution-processed synthesis techniques result in T_x being a non-uniform mixture of –OH, –F, and =O [30]. MXenes have attracted an ever-increasing attention from different research communities, including electrochemistry [31], electromagnetic wave absorption/shielding [32], catalysis [3], sensing [33], biomedicine [34], energy harvesting [35], and so on. This is because of their diverse and adaptable chemical, optical, electrical, mechanical, and optical properties [36]. It has also been studied that the structure and composition of MXene are crucial in determining these properties [37].

The MXene family is capable of producing materials with 2, 3, 4, or 5 atomic layers of transition metal. The final MXene structure is dependent on its MAX phase precursor(s) [6]. MXene compositions such as V_2CT_x [38], Nb_2C [39], $Ti_3C_2T_x$ [40], $V_4C_3T_x$ [38], and $Mo_4VC_4T_x$ [41] have been reported. Among all, $Ti_3C_2T_x$ has been widely explored and studied for different applications [6]. The type of MAX phase, synthesis conditions (temperature, concentration, and etching time), and choice of etching solution all contribute to the exfoliation degree and subsequent characteristics of MXenes [42]. Careful control and optimization of these factors are essential for tailoring the properties of MXenes for specific applications [43]. Various synthesis methods such as HF etching [30, 44], acid/fluoride salt or hydro-fluoride etching for in-situ production of HF [45–48], electrochemical etching [49], alkali etching [50], molten salt etching [51], chemical vapor deposition, and atomic layer deposition [52] have been explored. These approaches will result in different MXene structures and surface chemical states, which will have an impact on the overall behavior and performance of MXenes, as discussed in detail previously [53]. Thus, by utilizing the appropriate synthesis process, researchers can maximize the potential of MXenes and tailor their properties to suit a wide range of application [54, 55].

MXenes can be classified into different families based on the number of atomic layers [18]. Each family of MXenes is particularly noteworthy depends on the applications and their properties. MXenes can be further categorized into two distinct types based on their transition-metal composition [56]. The first category is known as mono-transition-metal (Mono-M) MXenes, in which the M layers consist of a single type of transition metal. Examples of Mono-M MXenes include Ti_2CT_x, V_2CT_x, $Ti_3C_2T_x$, $Nb_4C_3T_x$, and others. The second category is referred to as double transition-metal (DTM) MXenes. DTM MXenes are composed of two different transition metals, such as $Mo_2Ti_2C_3T_x$, $Mo_2TiC_2T_x$, and so on. DTM MXenes can also be classified based on their structure into two categories: ordered MXenes and solid-solution MXenes. Within the ordered MXenes, there are further classified into in-plane order and out-of-plane order [56].

https://doi.org/10.1007/s40820-024-01418-0

Number of reviews on MXenes, MXenes composites, DTM MXenes, etc. have already been published [5, 56–62] for various applications. It is highly desirable to describe this feature to better comprehend the development potential of MXene family based on the number of atomic layers they possess in the field of energy storage [63–66], specifically supercapacitors (SCs) [67–70]. M_3X_2 particularly Ti_3C_2 and M_2X and have been greatly explored among different MXenes based on the number of atomic layers [71]. In comparison, the M_5X_4 and M_4X_3 MXenes have received relatively less attention and are more challenging to synthesize. As of now, only a limited number of M_5X_4 MXenes have been synthesized, which means that comprehensive compilation and understanding of these materials as a review will require more time and research efforts [18]. Herein, we focused a review on M_4X_3 MXenes. M_4X_3 MXenes display exceptional electronic, magnetic, electrochemical, optical, and mechanical properties, making them stand out in the realm of 2D materials [71]. Benefited by its structural features, such MXene displayed enhanced oxidation resistance and improved electrochemical activity than its other MXene counterparts. For example, a previous report already demonstrated higher capacitance for $Ta_4C_3T_x$ MXene than $Ti_3C_2T_x$ and Ti_2CT_x MXenes [72]. Furthermore, $V_4C_3T_x$ MXene also exhibited higher specific capacitance than several $Ti_3C_2T_x$ MXene and related composites [68]. To date, there is currently no review specifically focused on M_4X_3 MXenes. This highlights the need for a comprehensive examination and analysis of the properties, applications, and potential future directions of M_4X_3 MXenes as shown in Fig. 1. Such a review would contribute significantly to the understanding and advancement of this unique class of 2D materials.

2 Overview of Supercapacitors

Energy storage devices are the pioneer of modern electronics world. Among, SCs have been widely studied because of their improved electrical performance including fast charge/discharge ability, enhanced power density, and long cycle life [73–75]. Based on the energy storage mechanism, supercapacitors classified principally into three main classes: Electric double layer capacitors (EDLCs), pseudocapacitors or redox capacitors (PCs), and hybrid capacitors (HCs) [76–80].

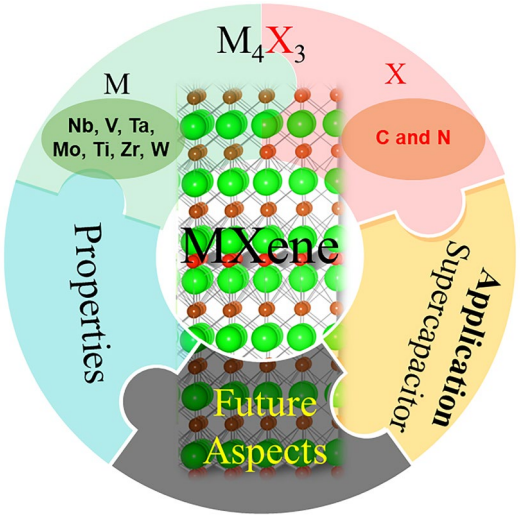

Fig. 1 Overview schematic of the review focus areas

EDLCs can store charges by non-faradaic electrochemical process i.e. electrostatically by forming electric double layer at electrode and electrolyte interface [81, 82]. An electrostatic charge storage is simple and fast as it stores charges on electrode surface without any charge transfer between the electrode and electrolyte ions. However, PCs store charges through Faradaic electrochemical process, wherein charge transfer occurs between the electrode and electrolyte. On the other hand, HCs following both the charge storage mechanism. While the carbon-based materials display the EDLC-type charge storage mechanism, the metal oxides generally follow the PC-type charge storage route [83, 84]. For achieving prominent electrochemical performance, any SC electrodes should have good conductivity, large surface area, and high porosity. MXene materials usually display PC-type charge storage mechanism [85–88]. For the common $Ti_3C_2T_x$ MXene, the presence of water molecules between the layers plays significant role on activating the redox reactions of the Ti atoms [89]. To improving the capacitive performance, MXenes have been systematically integrated with other carbon materials [90–92], metal oxides [93, 94], metal sulfides, hydroxides etc.

3 Expansion of the M_4X_3 MXene

Figure 2a illustrates the timeline of M_4X_3 MXenes, highlighting the substantial expansion of this MXene family since their discovery. New members have been added almost every year, showcasing the continuous growth of MXenes. However, when compared to M_2X the number

of publications on M_4X_3 MXenes low due to the complex synthesis approach. Nonetheless, there has been a recent increase in research interest towards M_4X_3 MXenes due to their fascinating properties. Ta_4C_3, Nb_4C_3, $Mo_2Ti_2C_3$ $(NbTi)_4C_3$, $(NbZr)_4C_3$, T_4N_3, V_4C_3, $(MoV)_4C_3$, $(TiTa)_4C_3$, and V_3CrC_3 have been successfully synthesized and investigated for various applications [18]. These materials have exhibited intriguing physicochemical properties in various studies. Although M_4X_3 MXenes have received less attention from researchers compared to M_2X and M_3X_2, Recent studies have revealed that M_4X_3 MXenes possess unique and compelling properties [68, 69, 95, 96]. This has sparked growing interest in exploring their potential applications and expanding our understanding of these materials. To date, over 50 stoichiometric MXenes have been experimentally synthesized in the lab [18]. These include various combinations of transition metals (M) and carbon/nitrogen (X) elements. Each stoichiometric MXene possesses distinct characteristics and potential applications. In addition to the experimentally synthesized MXenes, there are hundreds of MXene compositions that have been computationally predicted. These computationally predicted MXenes expand the possibilities for exploring novel materials with tailored properties. Downes et al. [18] summarized almost all the M_2X, M_3X_2, M_4X_3, and even the newly reported M_5X_4 MXenes as show in Fig. 2b. M_4X_3 MXene stands out from other MXenes due to its unique set of advantages, making it an attractive material for electrochemical energy storage devices. The $Nb_4C_3T_x$ MXene demonstrated impressive performance for Li-ion batteries due to their excellent electronic conductivity and large interlayer spacing which accommodated more lithium ions [97]. Further, it has garnered increasing attention due to its exceptional electrical and mechanical properties

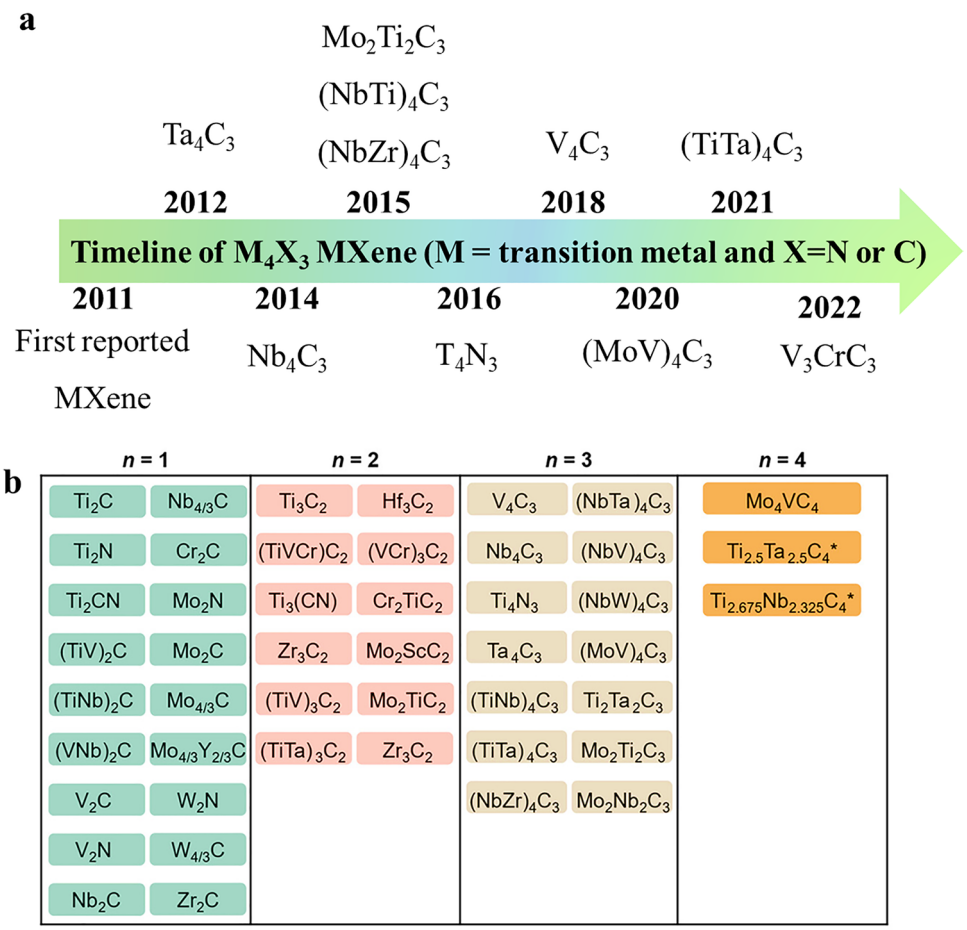

Fig. 2 **a** A brief timeline of the progress in M_4X_3 MXenes. **b** Synthesized MXenes reported to date, including 18 M_2X, 12 M_3X_2, 14 M_4X_3, and three M_5X_4. Reproduced with permission from Ref. [18]. Copyright 2023, American Chemical Society

https://doi.org/10.1007/s40820-024-01418-0

[98]. These combined factors motivated researcher to study $Nb_4C_3T_x$ for energy storage applications. For instance, V_4C_3 MXene possess greater interlayer spacing which facilitates the insertion and diffusion of ions during charging and discharging processes, leading to improved electrochemical performance. Furthermore, it also exhibits excellent structural durability, making it highly resistant to mechanical stress and deformation during battery operation. In addition to its mechanical properties and thermal stability, V_4C_3 MXene possesses tremendous metallic properties due to a narrow band gap at the Fermi level, making it highly conductive [99].

4 Properties and Advantages of MXene Appropriate for SCs

MXenes offer numerous excellent properties and advantages that make them highly attractive for various applications. Some key properties and advantages of MXenes are shown in Fig. 3.

4.1 Electronic Conductivity

The electronic conductivity of MXenes is influenced by various factors, including their composition, structure, surface groups, preparation conditions, and post-etching treatments [4, 57]. Increasing the surface area of MXenes and reducing defects are effective approaches to improving their conductivity [26, 100, 101]. The excellent electrical conductivity enables MXenes to be utilized in a wide range of applications, including sensors, thermal heaters, electromagnetic interference shielding, and energy storage [5, 59]. In the context of energy storage, MXenes can also serve as current collectors, establishing a conductive framework that enhances the electronic conductivity of electrode materials. Furthermore, when building electrodes or current collectors, this high conductivity might eliminate the need for extra conductive materials and binders, simplifying the manufacturing process and reducing costs. This conductivity enhancement facilitates efficient charge transport within the electrode, leading to improved performance in energy storage devices [102, 103]. The high surface area of MXene allows for a higher quantity of active sites available for charging/discharging, resulting in enhanced energy storage capacity.

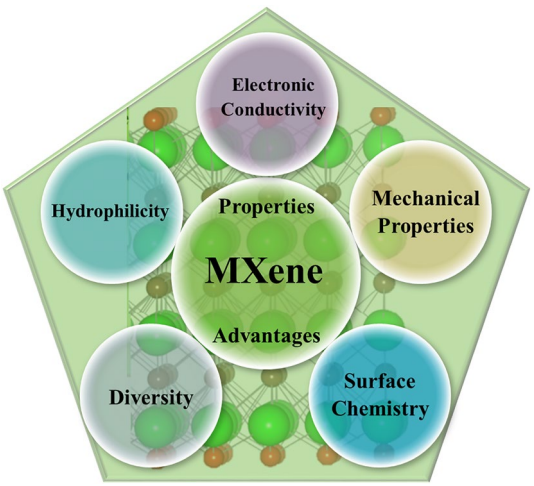

Fig. 3 Unique properties of MXene materials

4.2 Hydrophilicity

Hydrophilic surfaces have a strong affinity for water are preferred in the dispersion of water. The MXene ink need to be dispersed in different solvents for the fabrication of electrodes. The hydrophilicity of MXenes enable its compatibility with aqueous electrolytes. The stable hydrophilicity of MXene in aqueous solutions relies on the presence O and OH groups. The hydrophilic properties of MXene can be controlled by adjusting the surface terminations (OH, F, Cl, O) through specific synthesis techniques. Furthermore, the surface terminal groups of MXene play a significant role in determining the electrochemical performance of MXene-based electrodes for supercapacitors [104]. MXene can also be utilized as a current collector in other energy storage devices such as aqueous Zn-batteries. It has the possibility to achieve a uniform flux of Zn ions. This promotes homogenized Zn deposition, leading to improved battery performance [7]. Moreover, the hydrophilic properties of MXenes also make it interact favorably with polymer matrices. This beneficial interaction is particularly advantageous when MXenes are used in composite materials. Thus, the hydrophilic nature of MXenes contributes to their successful integration and utilization in composite materials [105].

4.3 Mechanical Properties

MXenes are highly promising materials for various devices due to their flexible nature and unique 2D-lamellar structure. MXene possesses outstanding mechanical properties attributed to the high binding strength of M–C/M–N bonds. MXenes have high tensile strength and elastic modulus. Even when MXene films are folded or bent into different shapes, they demonstrate outstanding mechanical flexibility without any noticeable damage [70, 106]. The strength of M–X bonds in MXenes can be assessed by examining their bond stiffness, which is determined by the bond energy and the length of the M–X bond. The bond stiffness provides insights into the theoretical mechanical properties of MXenes, such as Young's modulus [107]. The exceptional mechanical performance makes MXene films well-suited as current collector as well as active material in energy storage devices [108]. Further, there has been a growing demand for small and portable "micro-electronic" system devices where MXenes have shown significant advancements [109, 110]. Less than 5% of the extensive research conducted on MXenes since their discovery has been devoted to investigating their mechanical and tribological properties [111]. The detailed mechanical proprieties and tribological properties have been summarized previously [111].

4.4 Diversity

The MXene family offers a wide range of possibilities due to the combination of more than a dozen transition metal elements denoted as "M" and adjustable surface functional groups denoted as "T*x*." This diversity is further enriched by various processing steps that enable the construction of different macroscopic architectures of MXene. Examples of such architectures include powder, slurry, free-standing films, aerogels, hydrogels etc. [6, 57, 112]. Additionally, the morphology and structure of MXene can be modified and controlled, allowing further diversification. Moreover, based on the choice of the transition metal "M," MXene can be transformed into various derivatives through processes such as sulfurization, calcination, nitridation, selenization, sulfurization, and chlorination [113]. These transformations expand the variety of MXene-based materials even further, offering a broad range of possibilities for the development of novel MXene derivatives with unique properties for versatile applications.

4.5 Surface Chemistry

Density functional theory (DFT) studies on MXenes have shown that MXene structures are fully terminated with functional groups. A greater negative energy value suggests a stronger bonding between the surface termination groups and the transition metals in MXenes [100]. The combinations of surface functional groups on MXene depend on the specific preparation methods and post-processing routes. Using HF or in situ HF-forming etching methods results in MXene surfaces possess the termination groups such as –O, –OH, and –F [6, 32]. Molten salt etching methods can introduce various functional groups like –Cl, –S, –Te, –Br, and –I [114]. Furthermore, post-thermal treatment can lead to the formation of –N groups [115]. These functional groups play a significant role in determining the physical and chemical performance of MXene. Further, the surface terminations of MXenes play a crucial role in determining their physical and chemical properties. The specific types and positions of surface terminations have a significant impact on various features of MXenes. Altering the surface chemistry of MXenes can have a profound effect on their electrochemical properties. Further, it is possible to obtain enhanced electrochemical performance by tailoring the surface terminations, in energy storage systems [100, 116, 117]. The presence of highly electronegative functional groups enables the formation of advanced MXene-based materials through electrostatic interactions with materials possessing a positively charged surface.

MXene also possesses other interesting properties, such as thermal, chemical, and optical [58, 118, 119]. All these advantages of MXenes such as a 2D structure, high electrical conductivity, mechanical strength, chemical stability, tunable surface chemistry offer a wide range of compositions, energy storage capabilities, and versatile applications [120–123]. These properties make MXenes highly promising materials for numerous technological applications and research endeavors.

https://doi.org/10.1007/s40820-024-01418-0

5 M_4X_3 MXenes for Energy Storage Applications

MXenes exhibit a distinctive combination of metallic conductivity and hydrophilicity, making them highly attractive as electrode materials for supercapacitors [124]. Their metallic conductivity enables efficient charge transport, while their hydrophilic nature facilitates electrolyte penetration and ion diffusion, leading to enhanced electrochemical performance. Herein, the recent advancements on Mono-M and DTM MXenes have been discussed for SCs.

5.1 Ta- and Ta–Ti-based M_4X_3 MXenes

MXenes have demonstrated excellent performance as electrode materials, offering their potential for improving the energy storage capabilities of aqueous supercapacitors [68]. Recently, Syamsai et al. [72] reported Ta_4C_3 MXene synthesized through HF etching route. The Ta_4C_3 MXene involves the removal of the aluminum (Al) layer from its MAX phase precursor. The electrochemical performance of Ta_4C_3 MXene was evaluated using cyclic voltammetry (CV) in a 0.1 M H_2SO_4 electrolyte under standard conditions. The CV measurements were conducted at various potential windows, ranging from -0.2 to 1 V at a scan rate of 1 V s^{-1} in the three-electrode system. The CV curves demonstrated that the synthesized Ta_4C_3 MXene exhibited electrical double-layer capacitor (EDLC) behavior with quasi-pseudocapacitive characteristics, as shown in Fig. 4a. The same group reported double-ordered titanium tantalum carbide MXene nanosheets, based on $Ti_xTa_{4-x}C_3$ synthesized through same approach [125]. Comprehensive investigations involving phase, structural, and vibrational analyses were explored to confirmed the successful synthesis of MXene. The studies further revealed that the MXene layers exhibited a hexagonal crystal system. A specific capacitance of 200 F g^{-1} was achieved at a scan rate of 10 mV s^{-1} in two-electrode setup by using 1 M H_2SO_4. The CVs of the $Ti_xTa_{4-x}C_3$ were recorded at various potential windows, ranging from -0.2 to $+0.8$ V, using a scan rate of 1 V s^{-1} as shown in Fig. 4b. Such electrochemical measurement allowed the performance of the MXene material within the specified potential range. The CV curves provided insights into the redox processes and capacitance properties of $Ti_xTa_{4-x}C_3$, contributing to a better understanding of its electrochemical performance. Lopez et al. [126] combined both first-principles calculations and experimental measurements on the lithiation process in Ti_4C_3 and $Ti_2Ta_2C_3$ MXene electrode materials. The findings indicate the successful synthesis of $Ti_2Ta_2C_3$ MXene with an interlayer distance of 0.4 nm. The study demonstrated that the double-ordered $Ti_2Ta_2C_3$ MXene has the ability to store four times the amount of lithium compared to the pristine Ti_4C_3 MXene. This enhancement in lithium storage capacity highlights the potential of $Ti_2Ta_2C_3$ MXene for advanced energy storage applications.

In another study related to Ta metal, Rafieerad et al. [127] introduced a novel hybrid material composed of $Ta_4C_3T_x$ MXene-tantalum oxide (TTO) as supercapacitor electrodes. The step-by-step schematic illustrations for the synthesis and functionalization of the mixed-dimensional TTO nanocomposite is shown in Fig. 4c. An innovative fluorine-free etching method was used to prepare a TTO hybrid nanostructure from MAX phase. Such approach not only provides a more environmentally friendly alternative but also enables the controlled synthesis and functionalization of the TTO hybrid nanostructure. This hybrid structure demonstrated a surface area that was 20% higher than oxidized $Ta_4C_3T_x$. As a result, the hybrid material exhibited a volumetric capacitance of 447 F cm^{-3} at a scan rate of 1 mV s^{-1}. This finding highlights the potential of the $Ta_4C_3T_x$ MXene-TTO hybrid as a compatible and high-performance material for supercapacitor applications.

5.2 Nb-based M_4X_3 MXenes

Another representative M_4X_3 MXene, $Nb_4C_3T_x$ has garnered attention across various fields due to its excellent conductivity and mechanical strength. Its unique combination of properties makes $Nb_4C_3T_x$ a highly promising material for diverse applications, including energy storage, electronics, and structural engineering. The growing focus on $Nb_4C_3T_x$ underscores its potential to drive significant advancements in various industries. Zhao et al. [128] successfully delaminated and transformed $Nb_4C_3T_x$ MXene nanosheets into freestanding films, exhibiting an interlayer spacing of 1.77 nm. This interlayer spacing is larger compared to most previously reported MXenes. The freestanding $Nb_4C_3T_x$ films were then tested as electrodes in supercapacitor, demonstrated high volumetric capacitance of 1075, 687, and 506 F cm^{-3} recorded in 1 M H_2SO_4, 1 M KOH, and 1 M

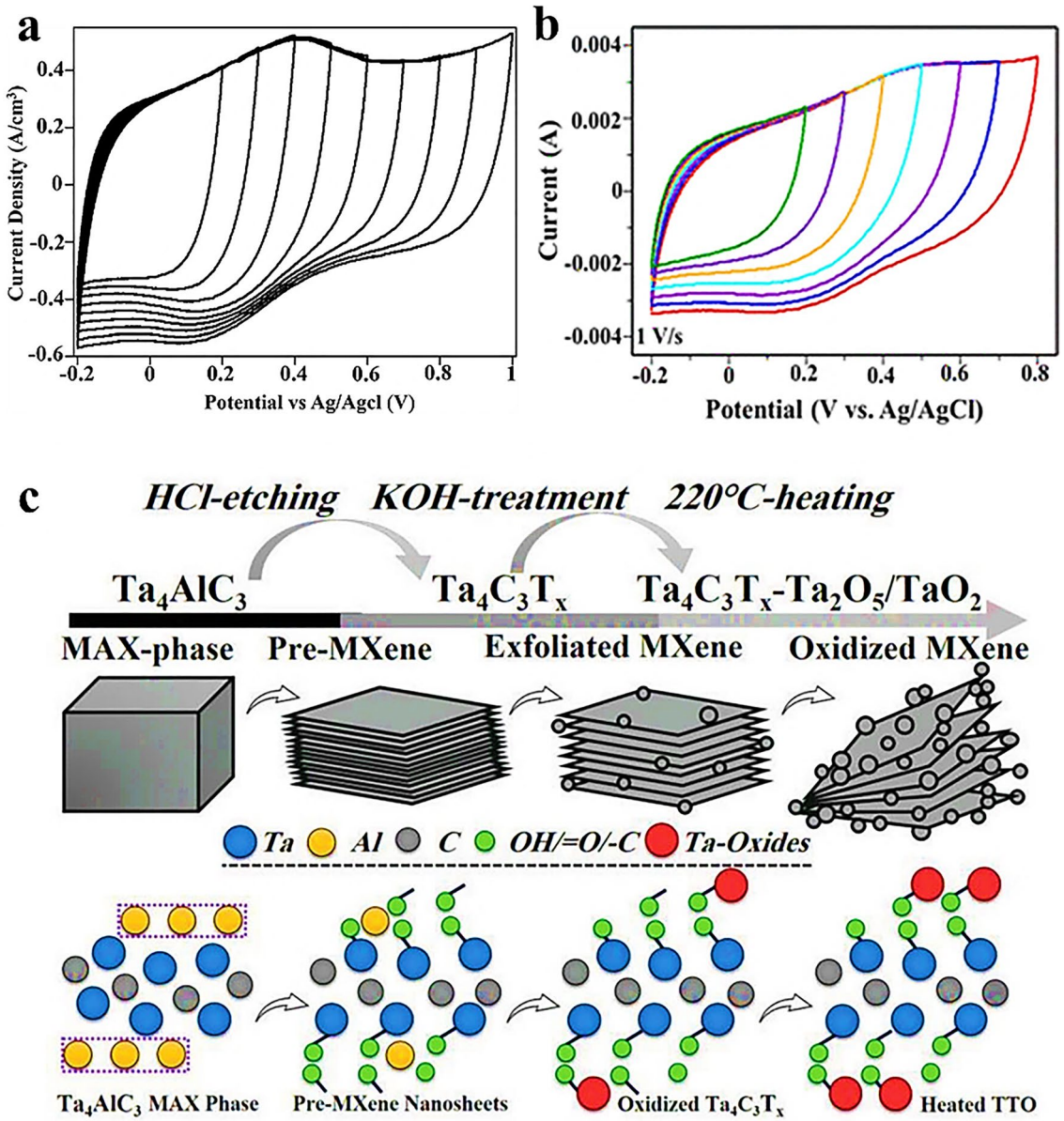

Fig. 4 **a** CVs at different potential windows at a scan rate of 1 V s^{-1}. Reproduced with permission from Ref. [72]. Copyright 2019, Elsevier; **b** CVs of MXene-$Ti_xTa_{4-x}C_3$ at different potential windows at a scan rate 1 V s^{-1}. Reproduced with permission from Ref. [125]. Copyright 2023, ACS Publications; and **c** step-by-step synthesis and schematic model and stoichiometry of TTO hybrid structure for the fluorine-free conversion of the Ta_4AlC_3 MAX phase to surface-modified $Ta_4C_3T_x$ MXene nanosheets decorated with tantalum oxide nanoparticles. Reproduced with permission from Ref. [127]. Copyright 2021, Wiley

$MgSO_4$ electrolytes, respectively, at a scan rate of 5 mV s^{-1}. To gain further insights into the structural changes occurring during the electrochemical charging process, an in-situ X-ray diffraction technique was employed as shown in Fig. 5a, b. The examination of the structural modifications of $Nb_4C_3T_x$ in 1 M H_2SO_4 and 1 M $MgSO_4$ electrolytes during the electrochemical charging process were carried out. During the electrochemical cycling process, it was observed that there was minimal change in the 21 Å interlayer spacing of the $Nb_4C_3T_x$ MXene. In the three charge–discharge cycles, the (002) peak associated with the interlayer spacing which did not exhibit significant movement in 1 M H_2SO_4 (Fig. 5a). This observation suggests that the interlayer spacing of 21 Å in $Nb_4C_3T_x$ MXene is sufficiently large to accommodate the

 https://doi.org/10.1007/s40820-024-01418-0

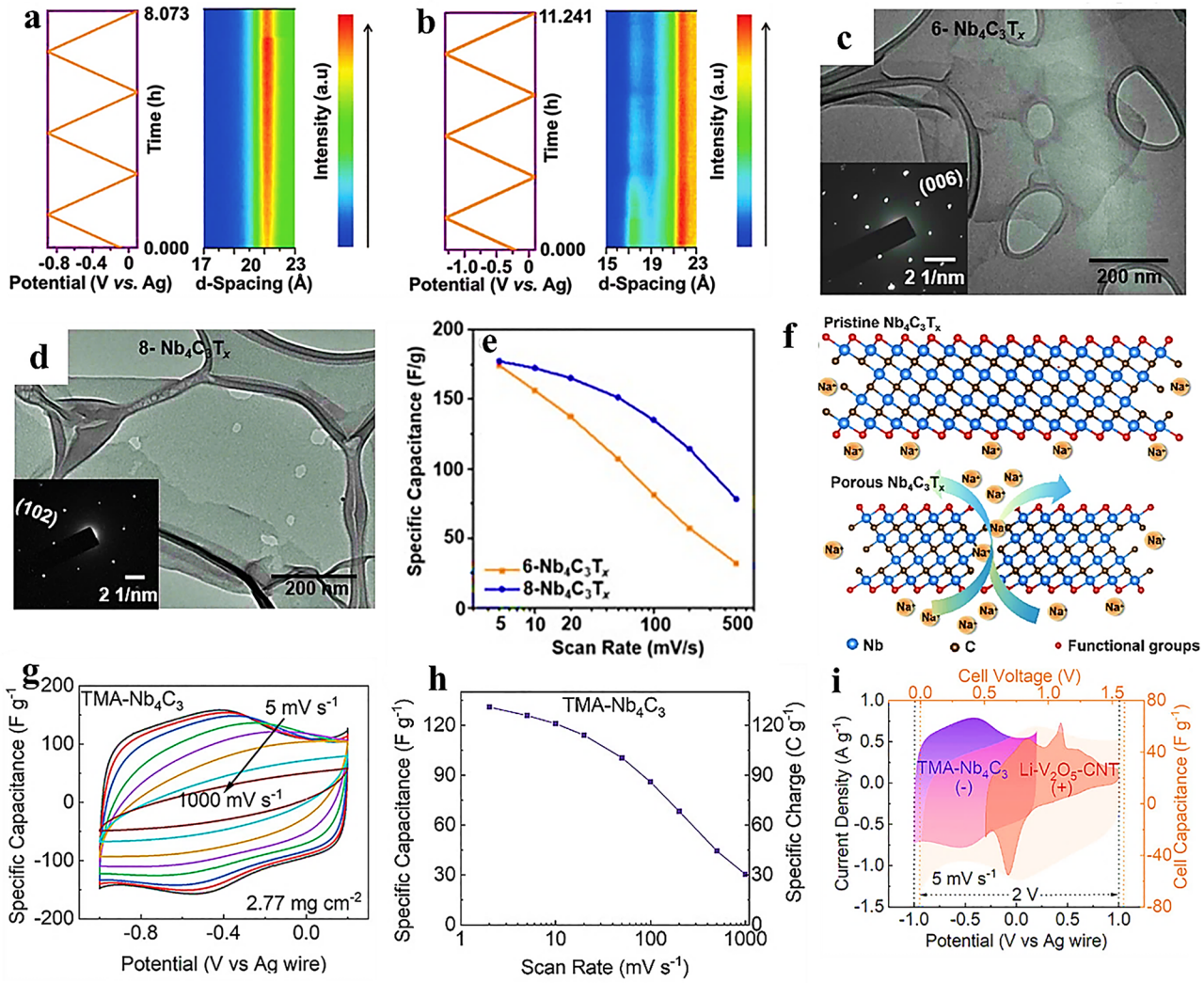

Fig. 5 In-situ XRD patterns during electrochemical cycles in **a** 1 m H_2SO_4 and **b** 1 m $MgSO_4$. Reproduced with permission from Ref. [128]. Copyright 2020 Wiley: TEM images of **c** 6-$Nb_4C_3T_x$, **d** 8-$Nb_4C_3T_x$ flakes. Inset shows SAED patterns, **e** variation of specific capacitance versus scan rate, and **f** schematic illustrating transport of electrolyte ions through $Nb_4C_3T_x$ layers and ion diffusion pathways between MXene sheets and across a $Nb_4C_3T_x$ flake with a pinhole. Reproduced with permission from Ref. [98]. Copyright 2022, Elsevier. **g** CVs of three-electrode cells containing a TMA-Nb_4C_3, **h** calculated specific capacitances of the TMA-Nb_4C_3 electrode as a function of scan rate, and **i** CVs of three-electrode cells containing Li-V_2C (− ve), Li-V_2O_5-CNT (+ ve) electrodes, and Li-V_2C/Li-V_2O_5-CNT asymmetric cell at 5 mV s^{-1}. Reproduced with permission from Ref. [67]. Copyright 2023, Wiley

intercalation of H^+ ions without causing lattice expansion. A similar phenomenon is observed in Fig. 5b, where the interlayer spacing of $Nb_4C_3T_x$ MXene in 1 M $MgSO_4$ solution is as high as 21.5 Å (2θ = 3.8°–5.8°). This suggests that the space between the MXene layers is ample to accommodate the insertion/deinsertion of cations. The stable interlayer spacing indicates that the MXene structure effectively accommodated the necessary structural changes associated with the electrochemical reactions during cycling, ensuring the stability and durability of the material. This behavior further supported the suitability of $Nb_4C_3T_x$ MXene for ion storage applications, as the interlayer spacing remains largely unchanged, allowing for efficient ion diffusion and reversible electrochemical processes. However, in the case of Mg^{2+} ions, their larger radius compared to H^+ ions allow them to gradually remove the TMAOH intercalant after numerous cycles. This results in a decrease in capacitance retention over time. Overall, the stable interlayer spacing in $Nb_4C_3T_x$ MXene enables efficient intercalation of H^+ ions, while the larger size of Mg^{2+} ions can lead to the removal

of intercalants, affecting the capacitance retention over extended cycling. The capacitive performance of $Nb_4C_3T_x$ MXene in neutral aqueous electrolytes has been previously reported as moderate, with limited efforts made to enhance it.

Zhao et al. [98] reported a novel method to enhance the capacitive performance by introducing nanopores (pinholes) into $Nb_4C_3T_x$ flakes through controlled etching time (6, 8, 10 days). The transmission electron microscopy (TEM) results (Fig. 5c, d) revealed that both samples exhibited transparent lamellar structures. The selective area electron diffraction (SAED) pattern displayed a distinct hexagonal structure, confirming the successful etching and delamination processes. In comparison to the smooth surface of the 6-$Nb_4C_3T_x$ sample, the 8-$Nb_4C_3T_x$ sample exhibited irregular pinholes on its surface. These pinholes were visually evident and indicated the introduction of nanopores in the material through the etching process. The presence of these pinholes suggested that the etching process was effective in generating the desired porous structure within the $Nb_4C_3T_x$ MXene, potentially leading to improved ion diffusion pathways and enhanced electrochemical performance. The etching process conducted for a duration of 10 days resulted in excessive flake damage, rendering the material fragile. Figure 5e provides a summary of the gravimetric capacitance of both the 6-$Nb_4C_3T_x$ and 8-$Nb_4C_3T_x$ films at various scan rates which were calculated based on CV curves in 1 M Li_2SO_4 medium. Both the 6-$Nb_4C_3T_x$ and 8-$Nb_4C_3T_x$ films exhibited capacitance values of 174 F g^{-1} (490 F cm^{-3}) and 177 F g^{-1} (equivalent to 485 F cm^{-3}), respectively, at a scan rate of 5 mV s^{-1}. Interestingly, when the scan rate is increased to 500 mV s^{-1}, the capacitance of the 8-$Nb_4C_3T_x$ film reaches 78 F g^{-1} (214 F cm^{-3}). This value is nearly 2.4 times higher than that of the 6-$Nb_4C_3T_x$ film, which exhibits a capacitance of around 32 F g^{-1} (90 F cm^{-3}) under the same scan rates. The resulting holey $Nb_4C_3T_x$ MXene exhibited a significant improvement in rate capability not only in 1 M Li_2SO_4 but also 1 M Na_2SO_4. This significant improvement in capacitance for the 8-$Nb_4C_3T_x$ film suggested that the introduction of pinholes through the etching process enhances the rate capability of the material. A schematic representation (Fig. 5f) of the electrode–electrolyte interface incorporating the findings from the aforementioned analysis. This schematic illustrated the impact of pinholes on the ion transport mechanism in MXene films. For the $Nb_4C_3T_x$ MXene without pinholes, ions in the electrolyte predominantly traverse through the gaps between the 2D layers. However, this transmission path is relatively long, potentially leading to slower ion diffusion and limiting the electrochemical performance. In contrast, the presence of pinholes in the $Nb_4C_3T_x$ MXene allows ions to not only move through the gaps between the layers but also more rapidly access the interior of the material through the pores. This additional pathway provided by the pinholes effectively shortens the ion transport distance, facilitating faster ion diffusion and leading to improved electrochemical performance, particularly at higher scan rates. The introduction of pinholes in $Nb_4C_3T_x$ MXene represents a promising approach to boost the capacitive performance of MXene materials in neutral aqueous electrolytes.

Recently, Mohit et al. [67] studied the electrochemical performance of TMA-Nb_4C_3 in 5 M LiCl. The CV results (Fig. 5g) within a potential window of -1 to $+0.2$ V of the TMA-Nb_4C_3 electrode were studied at various scan rates ranging from 5 to 1000 mV s^{-1}. The CV curves indicate the pseudocapacitive-behavior of the electrode. At lower scan rates, the CV curves show the presence of a pair of broad peaks in both the anodic and cathodic scans. These peaks were indicative of the redox reactions associated with the pseudocapacitive-behavior of the electrode material. The specific capacitance of the TMA-Nb_4C_3 electrode reached a maximum value of 131 F g^{-1} at a scan rate of 2 mV s^{-1}. The detailed specific capacitances at various scan rates have been illustrated in Fig. 5h. To expand the voltage window, an asymmetric cell using TMA-Nb_4C_3 (-1.0 to 0.2 V) and Li-V_2O_5-CNT (-0.3 to 1.0 V) electrodes were used to achieve favorable electrochemical performance for practical applications. A stable voltage window of 1.6 V was obtained which was lower than theoretical value. This discrepancy was due to the presence of overlapped junction regions in both the negative and positive electrodes (Li-V_2O_5-CNT and TMA-Nb_4C_3, respectively) within the TMA-Nb_4C_3/Li-V_2O_5-CNT asymmetric cell as shown in Fig. 5i. Despite this limitation, the asymmetric cell exhibited a capacitance of approximately 29 F g^{-1} at 1 A g^{-1}, demonstrating its potential for energy storage applications. Additionally, the asymmetric cell demonstrated excellent cyclability, with a high retention of approximately 95% after 10,000 cycles, indicating its long-term stability and durability.

https://doi.org/10.1007/s40820-024-01418-0

5.3 V-based M_4X_3 MXenes

The V_4C_3 MXene possesses expanded interlayer spacing and abundant redox active sites, indicating its potential as an electrode material. The enlarged interlayer spacing $V_4C_3T_x$ MXene allows easier ion intercalation and promotes efficient charge transport within the material. Additionally, the presence of numerous redox active sites provides additional pathways for charge transfer, further enhancing its electrical conductivity. Bin et al. [96] reported $V_4C_3T_x$ MXene to tackle with the stability and poor performance of compactly stacked layers-based electrode materials. The MAX phased of V-based MXene was transformed into multi-layered $V_4C_3T_x$ MXene, and then further delaminated to single layer nanoflakes (d-$V_4C_3T_x$) using tetra-n-butylammonium hydroxide (TBAOH). These delaminated nanoflakes had the capability to self-assemble into a flexible film without the need for a binder material. Figure 6a illustrated the schematic representation of the preparation process for the flexible and free-standing d-$V_4C_3T_x$ film. The resulting d-$V_4C_3T_x$ film exhibits a significant interlayer spacing of 2.1 nm. This enlarged spacing plays a crucial role in facilitating the diffusion of ions, allowing for reversible intercalation and deintercalation processes without causing damage to the layered structure. As a result, the d- d-$V_4C_3T_x$ film demonstrated excellent electrochemical performance, presenting its superior capabilities in energy storage and other electrochemical applications. The excellent cycle performance of the d-$V_4C_3T_x$ film electrode was studied through a repeated GCD cycles. The film electrode was subjected to 40,000 cycles at a high current density of 10 A g^{-1} and a wide potential window ranging from − 0.95 to − 0.15 V, retaining 93.1% of the capacitance (Fig. 6b). Even after an extended duration of 60,000 cycles, the capacitance retention remained 82.9%. Furthermore, the GCD cycles of the first and last ten cycles (60,000th cycle) are shown in the

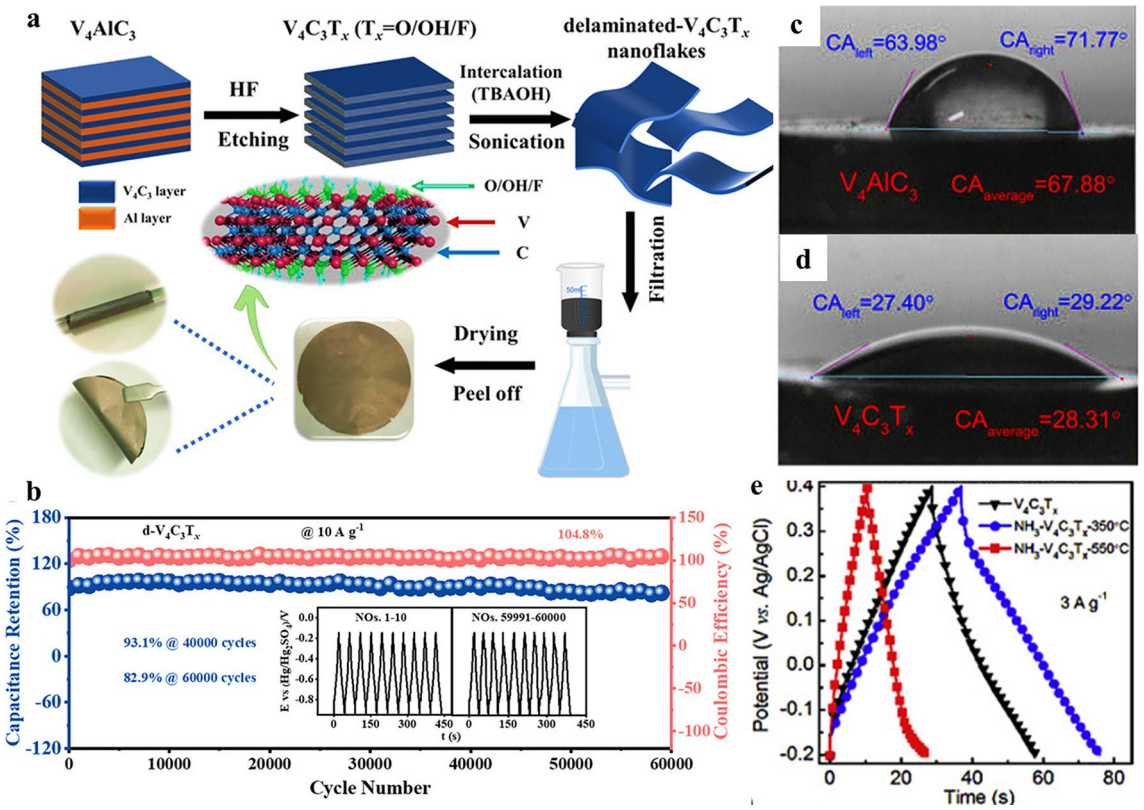

Fig. 6 **a** Preparation schematic for the d-$V_4C_3T_x$ film and **b** the d-$V_4C_3T_x$ film for 60,000 cycles (the inset shows the charge–discharge profiles from the first to 10th cycles and the last ten cycles for the 60,000th cycles). Reproduced with permission from Ref. [96]. Copyright 2022, Wiley. Photographs of the water droplet shape with the contact angle (CA) on cold-pressed free-standing discs of the ball-milled **c** V_4AlC_3 and **d** $V_4C_3T_x$. Reproduced with permission from Ref. [68]. Copyright 2019, Elsevier. **e** GCD curves of the $V_4C_3T_x$, NH_3-$V_4C_3T_x$-350 °C and NH_3-$V_4C_3T_x$-550 °C at 3 A g^{-1}. Reproduced with permission from Ref. [69]. Copyright 2019, Elsevier

inset of Fig. 6b. It was evident that the GCD curves before and after the cycles were nearly identical, indicating no significant deformation or deterioration in the electrode's performance. This observation further confirms the outstanding cycle reversibility demonstrated by the flexible d-$V_4C_3T_x$ film electrode.

Teng et al. [38] studied $V_4C_3T_x$ MXenes which exhibited a notable disparity in their performance between acidic and basic electrolytes. In acidic electrolytes, $V_4C_3T_x$ demonstrated a superior capacitance of 284 F g^{-1}, indicating its excellent energy storage capabilities. However, in basic electrolytes, its performance was comparatively moderate. $V_4C_3T_x$ MXenes showed significant electrochemical stability even after 60,000 cycles, highlighting maintained structural integrity these MXenes. In addition to large interlayer spacing, high specific surface areas and pore volumes, good conductivity etc. the hydrophilicity was also crucial factor to be measured when using MXenes as electrode materials for SCs. Thus, in the context of SC electrodes operating with aqueous electrolytes, the contact angle (CA) with water is a critical parameter to be considered. Wang et al. [68] measured the CA of the $V_4C_3T_x$ MXenes and its MAX phase surfaces (Fig. 6c, d). In the case of $V_4C_3T_x$ MXenes, the average contact angle was determined to be 28.31° which was much lower than the MAX phase V_4AlC_3 (67.88°), suggesting a greatly enhanced hydrophilic behavior. In other words, the as-synthesized $V_4C_3T_x$ MXene exhibits a stronger attraction to water, indicating a higher affinity for aqueous electrolytes, which was desirable for efficient supercapacitor performance. When employed as a supercapacitor electrode, the $V_4C_3T_x$ MXene material exhibited higher capacitance of approximately 209 F g^{-1} at a scan rate of 2 mV s^{-1}. The MXene electrode demonstrated a long-term cyclic stability of 97.23% after 10,000 cycles at a current density of 10 A g^{-1}. This signified the ability of MXenes and made it a reliable and durable option for SC applications in 1 M H_2SO_4 electrolyte. Li et al. [69] improved the $V_4C_3T_x$ MXenes performance through nitrogen doping at different annealing temperatures. The concentration of nitrogen in $V_4C_3T_x$ MXene was controlled and optimized by annealing temperatures. The MXene treated at 350 °C (NH_3-$V_4C_3T_x$-350 °C) exhibited a higher specific capacitance of 210 F g^{-1} compared to pristine and other doped $V_4C_3T_x$ MXene at a scan rate of 10 mV s^{-1} in 1 M H_2SO_4 electrolyte (Fig. 6e). Such study indicated that the nitrogen-doped MXene electrode has an improved ability to store electrical charge, leading to enhanced energy storage performance. Additionally, NH_3-$V_4C_3T_x$-350 °C also exhibited excellent cycling stability, indicating that its electrochemical performance remains consistent over multiple charge–discharge cycles.

5.4 Mo-Ti-based M_4X_3 MXenes

The greater the range of chemical compositions and structural complexities found in double transition metal MXenes. Thus, the exploration of mixed metallic MXenes, specifically out-of-plane ordered $Mo_2Ti_2C_3$, in energy storage applications has been a good choice which is also less explored due to the lack of redox activity in many electrolytes. To address these limitations and enhance the electrochemical properties, a promising strategy involves simultaneous structural modifications and the induction of intercalation pseudocapacitance in neutral electrolytes. By implementing such approach, it is possible to enhance the electrochemical performance of mixed metallic MXenes and unlock their potential for energy storage applications. Mohit et al. [129] presented a simple method for synthesizing partially oxidized $Mo_2Ti_2C_3$ MXene, noted as PO-$Mo_2Ti_2C_3$, which exhibits enhanced charge storage capability. A straightforward and efficient method was used for producing partially oxidized PO-$Mo_2Ti_2C_3$ through thermal annealing of pristine $Mo_2Ti_2C_3$ under mild conditions, as depicted in Fig. 7a. The structural analysis of PO-$Mo_2Ti_2C_3$ reveals the presence of pinholes, high roughness, and oxide nanostructures on the surface of the MXene. The free-standing films of PO-$Mo_2Ti_2C_3$ exhibit a rougher surface compared to smooth films of $Mo_2Ti_2C_3$ which display a more ordered structure. The comparative SEM images of pristine $Mo_2Ti_2C_3$ and PO-$Mo_2Ti_2C_3$ are depicted in Fig. 7b, c. The roughness observed in the PO-$Mo_2Ti_2C_3$ films can be attributed to the formation of the oxide layer upon heating. This structural difference between the two types of films highlights the impact of thermal oxidation on the surface characteristics and ordering of the MXene material.

These oxide nanostructures act as spacers, preventing the restacking of MXene sheets and facilitating improved intercalation of Li + ions between the layers of PO-$Mo_2Ti_2C_3$ in a 5 m LiCl electrolyte. As a result of the enhanced intercalation was observed and several improvements compared to pristine $Mo_2Ti_2C_3$. The charge storage

 https://doi.org/10.1007/s40820-024-01418-0

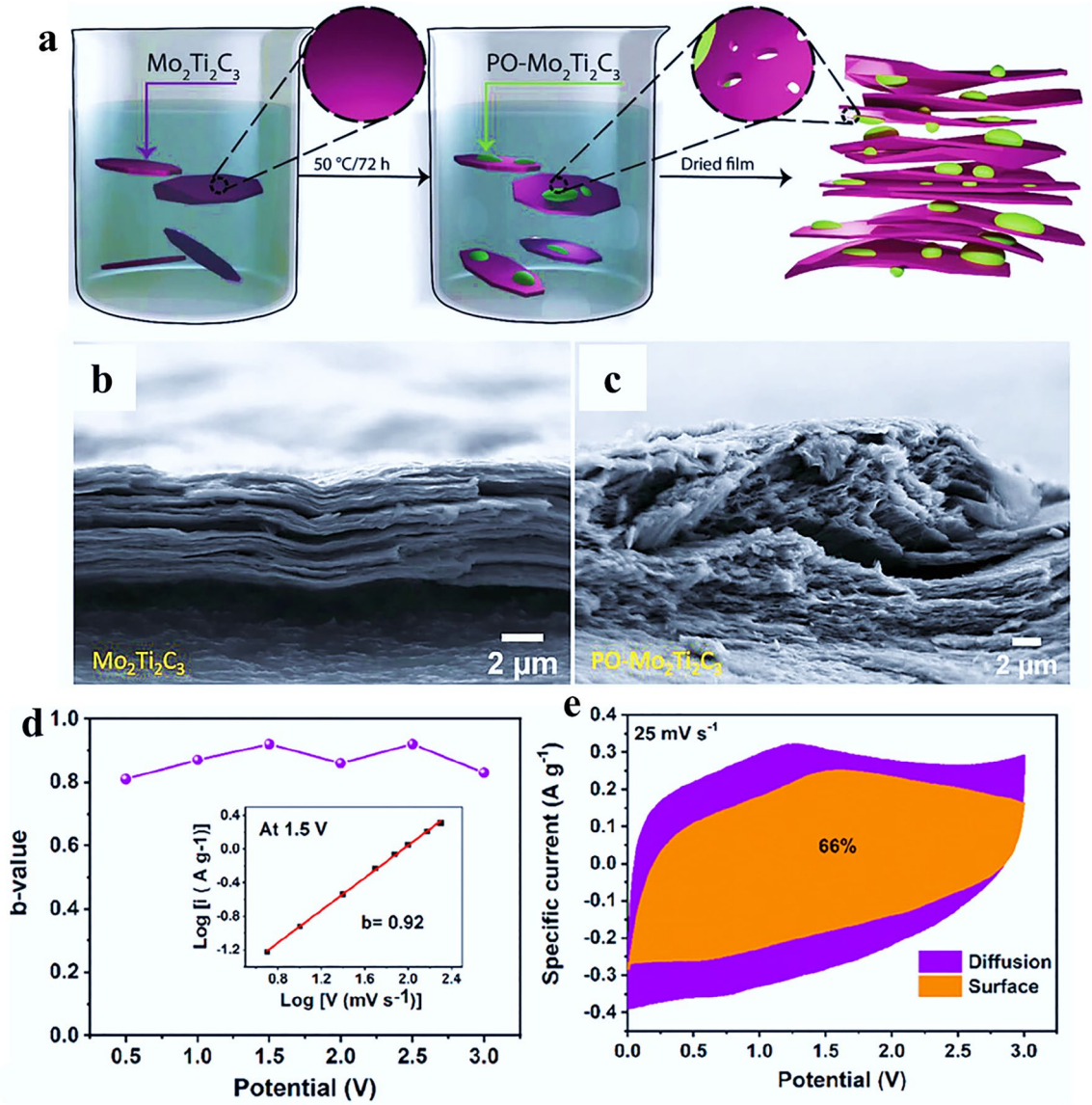

Fig. 7 **a** Schematic illustration of the synthesis of partially oxidized $Mo_2Ti_2C_3$ (PO-$Mo_2Ti_2C_3$), cross-sectional SEM images of **b** $Mo_2Ti_2C_3$ and **c** PO-$Mo_2Ti_2C_3$ free-standing MXene films. Reproduced with permission from Ref. [129]. Copyright 2023, Wiley. **d** Variation of *b*-values as a function of potential for the anodic scan. The inset shows the power–law dependence of the peak current at scan rates from 5 to 200 mV s^{-1}. **e** Percentage of the surface-controlled and diffusion-controlled area in the CV curve at a scan rate of 25 mV s^{-1} for f-$Mo_2Ti_2C_3$. Reproduced with permission from Ref. [130]. Copyright 2022, ACS Publications

capacity, cycle life, and Coulombic efficiency were all enhanced in PO-$Mo_2Ti_2C_3$. The formation of oxide nanostructures when $Mo_2Ti_2C_3$ was observed when subjected to thermal oxidation by using various optical, structural, and spectroscopic analyses. This indicates the potential of our approach to enhance the electrochemical performance of $Mo_2Ti_2C_3$-based materials for energy storage applications.

The energy density of supercapacitors is often limited by the narrow potential window in aqueous electrolytes. Ionic liquid electrolytes offer a higher potential window and superior specific energy but can be challenging due to slow ion transport and difficult intercalation caused by their larger ion size. Therefore, it is desirable to investigate MXenes with larger interlayer-spaced (*d*-spaced) structures that can

Table 1 M_4X_3 MXene electrode and device electrochemical performance for supercapacitors

M_4X_3 MXene	Electrolyte	Electrode/device performance		References
Composition	Aqueous/organic	Specific capacitance	Cycling stability/Retention%	
$Mo_2Ti_2C_3$	5 M LiCl	102 F g^{-1} at 5 mV s^{-1}	10,000/85	[129]
PO-$Mo_2Ti_2C_3$	5 M LiCl	132 F g^{-1} at 5 mV s^{-1}	10,000/100	[129]
f-$Mo_2Ti_2C_3$//f-$Mo_2Ti_2C_3$	1 M EMIMTFSI	152 F g^{-1}	5,000/86	[130]
$Mo_{2.7}V_{1.3}C_3$	1 M H_2SO_4	300 F g^{-1}	12,000/90	[131]
Zn//$V_3CrC_3T_x$	3 M $ZnSO_4$	397.5 F g^{-1}	50,000/70.2	[132]
$Ti_{2.9}Nb_{0.1}C_2T_x$	1 M H_2SO_4	104 F cm^{-3} at 2 mV s^{-1}	84,000/67.9	[133]
$Ti_xTa_{4-x}C_3$//$Ti_xTa_{4-x}C_3$	1 M H_2SO_4/PVA	200 F g^{-1}	30 days/80	[125]
$V_4C_3T_x$	1 M H_2SO_4	210 F g^{-1}	10,000/96.3	[69]
$V_4C_3T_x$	1 M H_2SO_4	330 F g^{-1}	3,000/90	[134]
V_4C_3	1 M H_2SO_4	209 F g^{-1}	10,000/97.23	[68]

facilitate the intercalation and deintercalation of larger ions. Gandla et al. [130] presented the $Mo_2Ti_2C_3$ MXene free-standing film electrode in a supercapacitor. 1M 1-ethyl-3-methylimidazolium bis(trifluoromethylsulfonyl)imide (EMIMTFSI) in acetonitrile electrolyte was utilized, which provides a wider potential window compared to aqueous electrolytes. The $Mo_2Ti_2C_3$ MXene electrode demonstrates excellent performance in this system, benefiting from the larger interlayer spacing that facilitates the intercalation and deintercalation process of the larger ions. The b-values ranged from 0.82 to 0.93 were obtained at various potentialsas depicted in Fig. 7d. These *b* values indicate the dominance of the surface-controlled capacitive process over intercalation pseudocapacitive. The surface-controlled capacitive current was approximately 66% of the total current at a scan rate of 25 mV s^{-1} for $Mo_2Ti_2C_3$ MXene (Fig. 7e). A significant increase was observed in the capacitive contributions at the higher scan rates, suggesting rapid charge transfer on the surface area. Further, Pinto et al. [131] have successfully synthesized and characterized four different compositions of $Mo_xV_{4-x}C_3$ with x values of 1, 1.5, 2, and 2.7. This study demonstrated that by adjusting the Mo: V ratio, surface terminations (O: F ratio) can be modified which tune the electrical and electrochemical properties of the resulting MXenes. Notably, the $Mo_{2.7}V_{1.3}C_3$ composition exhibited a volumetric capacitance up to 860 F cm^{-3}, and displayed high electrical conductivity of 830 S cm^{-1} at room temperature. Furthermore, these solid solution MXenes exhibited a wider range of positive potentials compared to other MXenes. Authors used $Mo_{2.7}V_{1.3}C_3$ as a positive electrode and combined it with a well-studied Ti_3C_2 MXene negative electrode to produce an all-MXene supercapacitor, demonstrating the potential of utilizing these tailored MXene compositions for high-performance energy storage applications. Further, Wang et al. [132] used a wet chemical etching method with hydrofluoric acid (HF) and successfully produced a solid-solution $V_{4-y}Cr_yC_3T_x$ ($y = 0$, 1, and 2) MXene derived from the solid-solution MAX phase. The addition of the Cr to second M-site metal brought a significant enhancement in the physiochemical properties of the $V_{4-y}Cr_yC_3T_x$ MXene, resulting improved electrochemical results. The electrochemical performance of such MXenes have been tabulated in Table 1.

Moreover, Huang et al. [71] reported the optimized synthesis strategy to obtain high-quality few-layer M_4X_3 MXenes (where M = V, Nb, Ta) that involves several key steps. These steps include precursor calcination, HF etching, intercalation, and exfoliation processes. By combining theoretical and computational analyses with experimental investigations, researchers can gain a comprehensive understanding of not only M_4X_3 MXenes but also other MXenes as well as their potential applications.

6 Conclusion and Future Aspects

In summary, this review highlights the recent advancements in M_4X_3 MXenes for supercapacitor electrode materials. The unique properties of 2D MXenes have also been discussed which offer several advantages over

https://doi.org/10.1007/s40820-024-01418-0

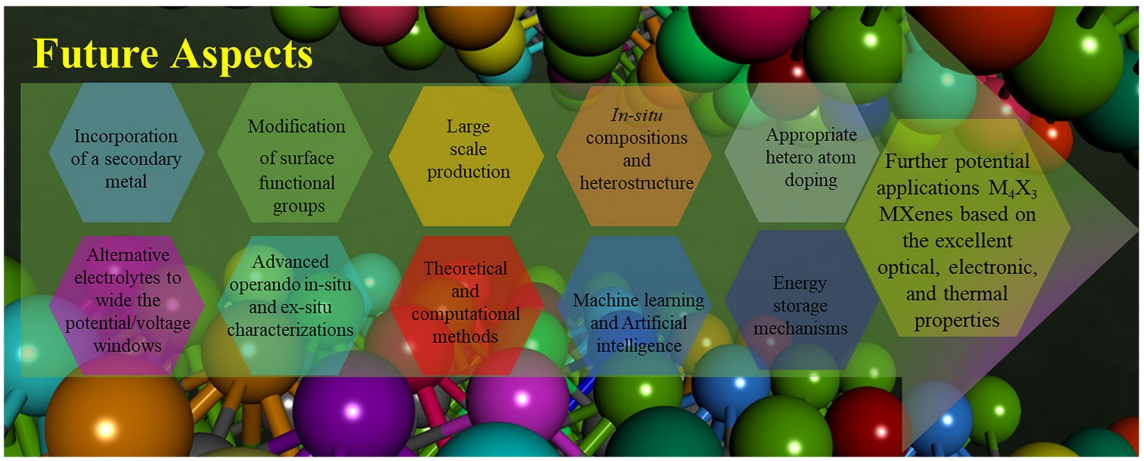

Fig. 8 Future directions of M_4X_3 MXenes

traditional materials as well as other MXenes. M_4X_3 have demonstrated excellent physicochemical properties, suggesting their potential for future advanced energy storage devices. However, there are still challenges to overcome in the research of M_4X_3-based electrode materials. Following futures aspects have been suggested:

- Incorporating a secondary metal along the early transitional metal group could further expand its properties to targeted applications. Introducing a secondary metal in MXene in the preparation stage of its initial MAX precursor can be beneficial. Apart from mono metal M_4X_3 MXene, it is important to explore the application of different compositions of double metal MXenes. Further, in the synthesis process, various surface functional groups can be introduced using different strategies for desired applications. For the discovery of new double transitional metal MXenes a new MAX phases are suggested to be studied.
- Effort should be directed towards the large scale the production of MXenes. However, it is essential to overcome challenges related to temperature regulation, mitigation of toxicity, and prevention of equipment corrosion.
- Indeed, exploring composite electrodes composed of MXenes holds great promise for energy storage applications. M_4X_3 MXenes can be further transformed to MXene in-situ composites and heterostructure without using other transition metal precursors [113]. Such heterostructured electrodes have the potential to harness the synergistic effects of the unique features offered by both 2D MXene and its composite materials. Further, the integration of hybrid structures could effectively enhance both electric double-layer capacitance (EDLC) and pseudocapacitance.
- Further potential applications M_4X_3 MXenes are suggested to be explored due to the excellent optical, electronic, and thermal properties.
- Surface engineering techniques, such as appropriate hetero atom doping and the synthesis of MXenes without particular terminations can be investigated to increase the interlayer spacing of MXene electrodes. This enhancement would enable improved electrochemical performance. A systematic exploration of functional groups and their impact on capacitance has the potential to open up new avenues for enhancing the performance of energy storage systems. Such investigation will help to find the materials with enhanced electrochemical behavior in energy storage applications.
- Alternative electrolytes to aqueous electrolytes with unique properties and wider electrochemical potential/voltage windows can be investigated to enable faster ion transport and create a safe and environmentally friendly environment for energy storage applications. Thus, exploring new electrolytes can potentially unlock new opportunities to enhance the overall performance of MXene materials in energy storage applications.
- It is evident that the complete covering or wrapping MXenes (especially M_4X_3 MXenes) with metal/metal oxide/metal sulfides are hindered due to the lack of flexibility in its structures. Such structural limitations effect the stability of the MXene-based electrode. To enhance the cycling stability, the construction of pillared structure with robust mechanical strength is highly recommended.

- Proper balance between the mechanical characteristics and the electrochemical properties is highly essential for any active materials in energy storage devices. In this aspect, defect-free MXenes (with less prone to oxidation) should be synthesized by following sophisticated synthetic routes.
- The current commercial current collectors still face several challenges. To overcome these limitations and achieve high-energy density in other energy storage devices such as batteries, exploring and designing innovative MXene based current could be a promising strategy. This approach might open up opportunities for advancing battery technology and improving overall battery performance.
- Advanced operando in-situ and ex-situ characterization techniques are indeed crucial for gaining a comprehensive understanding of the multi-functionalities of MXenes. This enables researchers to gain a thorough understanding of real-time observations and analyses of ion diffusion, charge transfer kinetics, and structural changes in MXene.
- Theoretical and computational methods are suggested to be employed. These methods play a significant role in understanding the properties and energy storage mechanisms of novel MXene and its hybrid materials.
- In MXenes with M_4X_3 composition and thicker layers, the M atoms in the inner layers are generally considered to be electrochemically inactive, in contrast to the M atoms in the outer layers. This should be further investigated to enhance the overall performance.
- The combination of advanced characterization techniques, theoretical/computational methods, and also machine learning and artificial intelligence offer a powerful approach for advancing the understanding and development of MXenes, ultimately leading to the design of improved energy storage devices.
- Green and cost-effective synthetic approaches for MXenes are highly essential in the light of current global situation and future electronics world. The detailed future suggestions are summarized in Fig. 8.

In summary, M_4X_3 MXene-based supercapacitors offer an exciting and promising properties to be explored. The purpose of this review is to give researchers a common platform to obtain information about the properties of M_4X_3 and its applications in supercapacitors. Additionally, this review offers suggestions to be considered in the future applications.

Acknowledgements This work was supported by the Hong Kong Research Grants Council (Project Number CityU 11218420). K.F.F express appreciation to the Deanship of Scientific Research at King Khalid University Saudi Arabia for funding through research groups program under Grant Number R.G.P. 2/593/44.

Declarations

Conflict of interest The authors declare no interest conflict. They have no known competing financial interests or personal relationships that could have appeared to influence the work reported in this paper.

References

1. A. Liu, X. Zhang, Z. Liu, Y. Li, X. Peng et al., The roadmap of 2D materials and devices toward chips. Nano-Micro Lett. **16**, 119 (2024). https://doi.org/10.1007/s40820-023-01273-5
2. C. Zhu, Y. Hao, H. Wu, M. Chen, B. Quan et al., Self-assembly of binderless MXene aerogel for multiple-scenario and responsive phase change composites with ultrahigh thermal energy storage density and exceptional electromagnetic interference shielding. Nano-Micro Lett. **16**, 57 (2023). https://doi.org/10.1007/s40820-023-01288-y
3. Z. Li, Y. Wu, 2D early transition metal carbides (MXenes) for catalysis. Small **15**, 1804736 (2019). https://doi.org/10.1002/smll.201804736
4. B. Anasori, M.R. Lukatskaya, Y. Gogotsi, 2D metal carbides and nitrides (MXenes) for energy storage. Nat. Rev. Mater. **2**, 16098 (2017). https://doi.org/10.1038/natrevmats.2016.98
5. F. Shahzad, A. Iqbal, H. Kim, C.M. Koo, 2D transition metal carbides (MXenes): applications as an electrically conducting material. Adv. Mater. **32**, 2002159 (2020). https://doi.org/10.1002/adma.202002159
6. C. Lamiel, I. Hussain, J.H. Warner, K. Zhang, Beyond Ti-based MXenes: a review of emerging non-Ti based metal-MXene structure, properties, and applications. Mater. Today **63**, 313–338 (2023). https://doi.org/10.1016/j.mattod.2023.01.020
7. M.S. Javed, A. Mateen, S. Ali, X. Zhang, I. Hussain et al., The emergence of 2D MXenes based Zn-ion batteries: recent

development and prospects. Small **18**, e2201989 (2022). https://doi.org/10.1002/smll.202201989

8. L. Lv, Z. Yang, K. Chen, C. Wang, Y. Xiong, 2D layered double hydroxides for oxygen evolution reaction: from fundamental design to application. Adv. Energy Mater. **9**, 1803358 (2019). https://doi.org/10.1002/aenm.201803358
9. F. Bonaccorso, Z. Sun, T. Hasan, A.C. Ferrari, Graphene photonics and optoelectronics. Nat. Photonics **4**, 611–622 (2010). https://doi.org/10.1038/nphoton.2010.186
10. Q.H. Wang, K. Kalantar-Zadeh, A. Kis, J.N. Coleman, M.S. Strano, Electronics and optoelectronics of two-dimensional transition metal dichalcogenides. Nat. Nanotechnol. **7**, 699–712 (2012). https://doi.org/10.1038/nnano.2012.193
11. K. Watanabe, T. Taniguchi, H. Kanda, Direct-bandgap properties and evidence for ultraviolet lasing of hexagonal boron nitride single crystal. Nat. Mater. **3**, 404–409 (2004). https://doi.org/10.1038/nmat1134
12. Y. Shao, J. Wang, H. Wu, J. Liu, I. Aksay et al., Graphene based electrochemical sensors and biosensors: a review. Electroanalysis **22**, 1027–1036 (2010). https://doi.org/10.1002/elan.200900571
13. M. Naguib, M. Kurtoglu, V. Presser, J. Lu, J. Niu et al., Two-dimensional nanocrystals produced by exfoliation of Ti_3AlC_2. Adv. Mater. **23**, 4248–4253 (2011). https://doi.org/10.1002/adma.201102306
14. S. Ajmal, A. Kumar, M. Selvaraj, M.M. Alam, Y. Yang et al., MXenes and their interfaces for the taming of carbon dioxide & nitrate: a critical review. Coord. Chem. Rev. **483**, 215094 (2023). https://doi.org/10.1016/j.ccr.2023.215094
15. K.A.U. Madhushani, A.A.P.R. Perera, A. Kumar, R.K. Gupta, MXene-based promising nanomaterials for electrochemical energy storage. Mol. Catal. **547**, 113284 (2023). https://doi.org/10.1016/j.mcat.2023.113284
16. A.A.P.R. Perera, K.A.U. Madhushani, B.T. Punchihewa, A. Kumar, R.K. Gupta, MXene-based nanomaterials for multifunctional applications. Materials **16**, 1138 (2023). https://doi.org/10.3390/ma16031138
17. V. Sharma, D. Kumar Das, R.K. Gupta, G. Yasin, A. Kumar, Synthesis strategies and structural and electronic properties of MXenes-based nanomaterials for ORR: a mini review. Inorg. Chem. Commun. **141**, 109496 (2022). https://doi.org/10.1016/j.inoche.2022.109496
18. M. Downes, C.E. Shuck, R.W. Lord, M. Anayee, M. Shekhirev et al., M_5X_4: a family of MXenes. ACS Nano **17**, 17158–17168 (2023). https://doi.org/10.1021/acsnano.3c04967
19. Y. An, Y. Tian, J. Feng, Y. Qian, MXenes for advanced separator in rechargeable batteries. Mater. Today **57**, 146–179 (2022). https://doi.org/10.1016/j.mattod.2022.06.006
20. Y. An, Y. Tian, Q. Man, H. Shen, C. Liu et al., Fluorine- and acid-free strategy toward scalable fabrication of two-dimensional MXenes for sodium-ion batteries. Nano Lett. **23**, 5217–5226 (2023). https://doi.org/10.1021/acs.nanolett.3c01201
21. Y. An, Y. Tian, H. Shen, Q. Man, S. Xiong et al., Two-dimensional MXenes for flexible energy storage devices. Energy Environ. Sci. **16**, 4191–4250 (2023). https://doi.org/10.1039/d3ee01841e
22. Y. Tian, Y. An, J. Feng, Y. Qian, MXenes and their derivatives for advanced aqueous rechargeable batteries. Mater. Today **52**, 225–249 (2022). https://doi.org/10.1016/j.mattod.2021.11.021
23. H. Ma, H. Fang, X. Xie, Y. Liu, H. Tian et al., Optoelectronic synapses based on MXene/violet phosphorus van der waals heterojunctions for visual-olfactory crossmodal perception. Nano-Micro Lett. **16**, 104 (2024). https://doi.org/10.1007/s40820-024-01330-7
24. W. Yu, Y. Yang, Y. Wang, L. Hu, J. Hao et al., Versatile MXene gels assisted by brief and low-strength centrifugation. Nano-Micro Lett. **16**, 94 (2024). https://doi.org/10.1007/s40820-023-01302-3
25. A. Zarepour, S. Ahmadi, N. Rabiee, A. Zarrabi, S. Iravani, Self-healing MXene- and graphene-based composites: properties and applications. Nano-Micro Lett. **15**, 100 (2023). https://doi.org/10.1007/s40820-023-01074-w
26. A. VahidMohammadi, J. Rosen, Y. Gogotsi, The world of two-dimensional carbides and nitrides (MXenes). Science **372**, eabf1581 (2021). https://doi.org/10.1126/science.abf1581
27. M.S. Javed, X. Zhang, T. Ahmad, M. Usman, S.S. Ahmad Shah et al., MXenes to MBenes: latest development and opportunities for energy storage devices. Mater. Today. (2024). https://doi.org/10.1016/j.mattod.2024.01.001
28. I. Hussain, U. Amara, F. Bibi, A. Hanan, M.N. Lakhan et al., Mo-based MXenes: synthesis, properties, and applications. Adv. Colloid Interface Sci. **324**, 103077 (2024). https://doi.org/10.1016/j.cis.2023.103077
29. X. Zhang, M.S. Javed, S. Ali, A. Ahmad, S.S. Ahmad Shah et al., Band engineering in $Ti_2N/Ti_3C_2T_x$-MXene interface to enhance the performance of aqueous NH_4^+-ion hybrid supercapacitors. Nano Energy **120**, 109108 (2024). https://doi.org/10.1016/j.nanoen.2023.109108
30. M. Alhabeb, K. Maleski, B. Anasori, P. Lelyukh, L. Clark et al., Guidelines for synthesis and processing of two-dimensional titanium carbide ($Ti_3C_2T_x$ MXene). Chem. Mater. **29**, 7633–7644 (2017). https://doi.org/10.1021/acs.chemmater.7b02847
31. L. Wang, M. Han, C.E. Shuck, X. Wang, Y. Gogotsi, Adjustable electrochemical properties of solid-solution MXenes. Nano Energy **88**, 106308 (2021). https://doi.org/10.1016/j.nanoen.2021.106308
32. F. Shahzad, M. Alhabeb, C.B. Hatter, B. Anasori, S. Man Hong et al., Electromagnetic interference shielding with 2D transition metal carbides (MXenes). Science **353**, 1137–1140 (2016). https://doi.org/10.1126/science.aag2421
33. S.J. Kim, H.-J. Koh, C.E. Ren, O. Kwon, K. Maleski et al., Metallic $Ti_3C_2T_x$ mxene gas sensors with ultrahigh signal-to-noise ratio. ACS Nano **12**(2), 986–993 (2018). https://doi.org/10.1021/acsnano.7b07460

34. K. Huang, Z. Li, J. Lin, G. Han, P. Huang, Two-dimensional transition metal carbides and nitrides (MXenes) for biomedical applications. Chem. Soc. Rev. **47**, 5109–5124 (2018). https://doi.org/10.1039/C7CS00838D
35. A. Agresti, A. Pazniak, S. Pescetelli, A. Di Vito, D. Rossi et al., Titanium-carbide MXenes for work function and interface engineering in perovskite solar cells. Nat. Mater. **18**, 1228–1234 (2019). https://doi.org/10.1038/s41563-019-0478-1
36. X. Li, Z. Huang, C.E. Shuck, G. Liang, Y. Gogotsi et al., MXene chemistry, electrochemistry and energy storage applications. Nat. Rev. Chem. **6**, 389–404 (2022). https://doi.org/10.1038/s41570-022-00384-8
37. J.L. Hart, K. Hantanasirisakul, A.C. Lang, B. Anasori, D. Pinto et al., Control of MXenes' electronic properties through termination and intercalation. Nat. Commun. **10**, 522 (2019). https://doi.org/10.1038/s41467-018-08169-8
38. T. Zhang, K. Matthews, A. VahidMohammadi, M. Han, Y. Gogotsi, Pseudocapacitance of vanadium carbide MXenes in basic and acidic aqueous electrolytes. ACS Energy Lett. **7**, 3864–3870 (2022). https://doi.org/10.1021/acsenergylett.2c01508
39. A. Byeon, A.M. Glushenkov, B. Anasori, P. Urbankowski, J. Li et al., Lithium-ion capacitors with 2D Nb_2CT_x (MXene)–carbon nanotube electrodes. J. Power. Sour. **326**, 686–694 (2016). https://doi.org/10.1016/j.jpowsour.2016.03.066
40. X. Wang, T.S. Mathis, Y. Sun, W.-Y. Tsai, N. Shpigel et al., Titanium carbide MXene shows an electrochemical anomaly in water-in-salt electrolytes. ACS Nano **15**, 15274–15284 (2021). https://doi.org/10.1021/acsnano.1c06027
41. G. Deysher, C.E. Shuck, K. Hantanasirisakul, N.C. Frey, A.C. Foucher et al., Synthesis of Mo_4VAlC_4 MAX phase and two-dimensional Mo_4VC_4 MXene with five atomic layers of transition metals. ACS Nano **14**, 204–217 (2020). https://doi.org/10.1021/acsnano.9b07708
42. M.S. Javed, A. Mateen, I. Hussain, A. Ahmad, M. Mubashir et al., Recent progress in the design of advanced MXene/metal oxides-hybrid materials for energy storage devices. Energy Storage Mater. **53**, 827–872 (2022). https://doi.org/10.1016/j.ensm.2022.10.005
43. O. Mashtalir, M. Naguib, B. Dyatkin, Y. Gogotsi, M.W. Barsoum, Kinetics of aluminum extraction from Ti_3AlC_2 in hydrofluoric acid. Mater. Chem. Phys. **139**, 147–152 (2013). https://doi.org/10.1016/j.matchemphys.2013.01.008
44. L. Verger, C. Xu, V. Natu, H.-M. Cheng, W. Ren et al., Overview of the synthesis of MXenes and other ultrathin 2D transition metal carbides and nitrides. Curr. Opin. Solid State Mater. Sci. **23**, 149–163 (2019). https://doi.org/10.1016/j.cossms.2019.02.001
45. M. Ghidiu, M.R. Lukatskaya, M.-Q. Zhao, Y. Gogotsi, M.W. Barsoum, Conductive two-dimensional titanium carbide 'clay' with high volumetric capacitance. Nature **516**, 78–81 (2014). https://doi.org/10.1038/nature13970
46. J. Halim, M.R. Lukatskaya, K.M. Cook, J. Lu, C.R. Smith et al., Transparent conductive two-dimensional titanium carbide epitaxial thin films. Chem. Mater. **26**, 2374–2381 (2014). https://doi.org/10.1021/cm500641a
47. F. Liu, A. Zhou, J. Chen, J. Jia, W. Zhou et al., Preparation of Ti_3C_2 and Ti_2C MXenes by fluoride salts etching and methane adsorptive properties. Appl. Surf. Sci. **416**, 781–789 (2017). https://doi.org/10.1016/j.apsusc.2017.04.239
48. X. Wang, C. Garnero, G. Rochard, D. Magne, S. Morisset et al., A new etching environment (FeF_3/HCl) for the synthesis of two-dimensional titanium carbide MXenes: a route towards selective reactivity vs.water. J. Mater. Chem. A **5**, 22012–22023 (2017). https://doi.org/10.1039/c7ta01082f
49. Y. Liu, T. Gao, H. Xiao, W. Guo, B. Sun et al., One-pot synthesis of rice-like TiO_2/graphene hydrogels as advanced electrodes for supercapacitors and the resulting aerogels as high-efficiency dye adsorbents. Electrochim. Acta **229**, 239–252 (2017). https://doi.org/10.1016/j.electacta.2017.01.142
50. J. Xuan, Z. Wang, Y. Chen, D. Liang, L. Cheng et al., Organic-base-driven intercalation and delamination for the production of functionalized titanium carbide nanosheets with superior photothermal therapeutic performance. Angew. Chem. Int. Ed. **55**, 14569–14574 (2016). https://doi.org/10.1002/anie.201606643
51. P. Urbankowski, B. Anasori, T. Makaryan, D. Er, S. Kota et al., Synthesis of two-dimensional titanium nitride Ti_4N_3 (MXene). Nanoscale **8**, 11385–11391 (2016). https://doi.org/10.1039/C6NR02253G
52. Y. Gogotsi, Chemical vapour deposition: transition metal carbides go 2D. Nat. Mater. **14**, 1079–1080 (2015). https://doi.org/10.1038/nmat4386
53. M. Hu, H. Zhang, T. Hu, B. Fan, X. Wang et al., Emerging 2D MXenes for supercapacitors: status, challenges and prospects. Chem. Soc. Rev. **49**, 6666–6693 (2020). https://doi.org/10.1039/d0cs00175a
54. C. Wei, Y. Wang, Y. Zhang, L. Tan, Y. Qian et al., Flexible and stable 3D lithium metal anodes based on self-standing MXene/COF frameworks for high-performance lithium-sulfur batteries. Nano Res. **14**, 3576–3584 (2021). https://doi.org/10.1007/s12274-021-3433-9
55. C. Wei, B. Xi, P. Wang, Y. Liang, Z. Wang et al., In situ anchoring ultrafine ZnS nanodots on 2D MXene nanosheets for accelerating polysulfide redox and regulating Li plating. Adv. Mater. **35**, e2303780 (2023). https://doi.org/10.1002/adma.202303780
56. W. Hong, B.C. Wyatt, S.K. Nemani, B. Anasori, Double transition-metal MXenes: Atomistic design of two-dimensional carbides and nitrides. MRS Bull. **45**, 850–861 (2020). https://doi.org/10.1557/mrs.2020.251
57. U. Amara, I. Hussain, M. Ahmad, K. Mahmood, K. Zhang, 2D MXene-based biosensing: a review. Small **19**, 2205249 (2023). https://doi.org/10.1002/smll.202205249
58. X. Wang, H. Li, H. Li, S. Lin, W. Ding et al., 2D/2D 1T-MoS_2/Ti_3C_2 MXene heterostructure with excellent supercapacitor performance. Adv. Funct. Mater. **30**, 1910302 (2020). https://doi.org/10.1002/adfm.201910302

 https://doi.org/10.1007/s40820-024-01418-0

59. M. Naguib, V.N. Mochalin, M.W. Barsoum, Y. Gogotsi, 25th anniversary article: MXenes: a new family of two-dimensional materials. Adv. Mater. **26**, 992–1005 (2014). https://doi.org/10.1002/adma.201304138
60. D. Huang, H. Kim, G. Zou, X. Xu, Y. Zhu et al., All-mxene thermoelectric nanogenerator. Mater. Today Energy **29**, 101129 (2022). https://doi.org/10.1016/j.mtener.2022.101129
61. I. Hussain, C. Lamiel, M.S. Javed, M. Ahmad, S. Sahoo et al., MXene-based heterostructures: current trend and development in electrochemical energy storage devices. Prog. Energy Combust. Sci. **97**, 101097 (2023). https://doi.org/10.1016/j.pecs.2023.101097
62. J. Jiang, F. Li, J. Zou, S. Liu, J. Wang et al., Three-dimensional MXenes heterostructures and their applications. Sci. China Mater. **65**, 2895–2910 (2022). https://doi.org/10.1007/s40843-022-2186-0
63. Y. Li, Z. Yuan, D. Li, J. Li, Y. Zhang et al., Multi-interface combination of bimetallic selenide and $V_4C_3T_x$ MXene for high-rate and ultrastable sodium storage devices. ACS Nano **18**, 4733–4745 (2024). https://doi.org/10.1021/acsnano.3c07977
64. Q. Lin, L. Wang, Layered double hydroxides as electrode materials for flexible energy storage devices. J. Semicond. **44**, 041601 (2023). https://doi.org/10.1088/1674-4926/44/4/041601
65. X. Xiao, L. Zhang, W. Xin, M. Yang, Y. Geng et al., Self-assembled layer of organic phosphonic acid enables highly stable MnO_2 cathode for aqueous znic batteries. Small (2024). https://doi.org/10.1002/smll.202309271
66. Z. Yuan, Q. Lin, Y. Li, W. Han, L. Wang, Effects of multiple ion reactions based on a $CoSe_2$/MXene cathode in aluminum-ion batteries. Adv. Mater. Deerfield Beach Fla **35**, e2211527 (2023). https://doi.org/10.1002/adma.202211527
67. M. Saraf, T. Zhang, T. Averianov, C.E. Shuck, R.W. Lord et al., Vanadium and niobium MXenes-bilayered V_2O_5 asymmetric supercapacitors. Small Meth. **7**, e2201551 (2023). https://doi.org/10.1002/smtd.202201551
68. X. Wang, S. Lin, H. Tong, Y. Huang, P. Tong et al., Two-dimensional V_4C_3 MXene as high performance electrode materials for supercapacitors. Electrochim. Acta **307**, 414–421 (2019). https://doi.org/10.1016/j.electacta.2019.03.205
69. H. Li, X. Wang, H. Li, S. Lin, B. Zhao et al., Capacitance improvements of V_4C_3T by NH_3 annealing. J. Alloys Compd. **784**, 923–930 (2019). https://doi.org/10.1016/j.jallcom.2019.01.111
70. M. Hu, Z. Li, G. Li, T. Hu, C. Zhang et al., All-solid-state flexible fiber-based MXene supercapacitors. Adv. Mater. Technol. **2**, 1700143 (2017). https://doi.org/10.1002/admt.201700143
71. Y. Huang, J. Shen, S. Lin, W. Song, X. Zhu et al., Defect-free few-layer $M_4C_3T_x$ (M=V, Nb, Ta) MXene nanosheets: synthesis, characterization, and physicochemical properties. Adv. Sci. **10**, 2302882 (2023). https://doi.org/10.1002/advs.202302882
72. R. Syamsai, A.N. Grace, Ta_4C_3 MXene as supercapacitor electrodes. J. Alloys Compd. **792**, 1230–1238 (2019). https://doi.org/10.1016/j.jallcom.2019.04.096
73. S. Sahoo, R. Kumar, E. Joanni, R.K. Singh, J.-J. Shim, Advances in pseudocapacitive and battery-like electrode materials for high performance supercapacitors. J. Mater. Chem. A **10**, 13190–13240 (2022). https://doi.org/10.1039/d2ta02357a
74. N.A. Salleh, S. Kheawhom, N. Ashrina, A. Hamid, W. Rahiman, A.A. Mohamad, Electrode polymer binders for supercapacitor applications: a review. J. Mater. Res. Technol. **23**, 3470–3491 (2023). https://doi.org/10.1016/j.jmrt.2023.02.013
75. I. Melkiyur, Y. Rathinam, P.S. Kumar, A. Sankaiya, S. Pitchaiya et al., A comprehensive review on novel quaternary metal oxide and sulphide electrode materials for supercapacitor: origin, fundamentals, present perspectives and future aspects. Renew. Sustain. Energy Rev. **173**, 113106 (2023). https://doi.org/10.1016/j.rser.2022.113106
76. S. Mirzazadeh Khomambazari, P. Lokhande, S. Padervand, N.D. Zaulkiflee, M. Irandoost et al., A review of recent progresses on nickel oxide/carbonous material composites as supercapacitor electrodes. J. Compos. Compd. **4**, 195–208 (2022). https://doi.org/10.52547/jcc.4.4.4
77. N. Lakal, S. Dubal, P.E. Lokhande, Chapter 22-Supercapacitors: an introduction, in *Micro and nano technologies, nanotechnology in the automotive industry*. ed. by T.A. Nguyen, G. Yasin, N.B. Singh, R.K. Gupta (Elsevier, Amsterdam, 2022), pp.459–466. https://doi.org/10.1016/b978-0-323-90524-4.00022-0
78. P. Lokhande, U. Chavan, S. Bhosale, A. Kalam, S. Deokar, Chapter 11-New-generation materials for flexible supercapacitors, in *Flexible supercapacitor nanoarchitectonics*. ed. by M.I. Ahamed, R. Boddula, T. Altalhi (Wiley, New York, 2021), pp.277–313. https://doi.org/10.1002/9781119711469.ch11
79. P.E. Lokhande, A. Pakdel, H.M. Pathan, D. Kumar, D.-V.N. Vo et al., Prospects of MXenes in energy storage applications. Chemosphere **297**, 134225 (2022). https://doi.org/10.1016/j.chemosphere.2022.134225
80. P.E. Lokhande, U.S. Chavan, A. Pandey, Materials and fabrication methods for electrochemical supercapacitors: overview. Electrochem. Energy Rev. **3**, 155–186 (2020). https://doi.org/10.1007/s41918-019-00057-z
81. I. Hussain, S. Sahoo, D. Mohapatra, M. Ahmad, S. Iqbal et al., Recent progress in trimetallic/ternary-metal oxides nanostructures: misinterpretation/misconception of electrochemical data and devices. Appl. Mater. Today **26**, 101297 (2022). https://doi.org/10.1016/j.apmt.2021.101297
82. I. Hussain, C. Lamiel, M. Ahmad, Y. Chen, S. Shuang et al., High entropy alloys as electrode material for supercapacitors: a review. J. Energy Storage **44**, 103405 (2021). https://doi.org/10.1016/j.est.2021.103405
83. I. Hussain, C. Lamiel, S. Sahoo, M.S. Javed, M. Ahmad et al., Animal- and human-inspired nanostructures as supercapacitor electrode materials: a review.

Nano-Micro Lett. **14**, 199 (2022). https://doi.org/10.1007/s40820-022-00944-z

84. Q. Liu, L. Liu, Y. Zheng, M. Li, B. Ding et al., On-demand engineerable visible spectrum by fine control of electrochemical reactions. Natl. Sci. Rev. **11**, nwad323 (2023). https://doi.org/10.1093/nsr/nwad323
85. I. Hussain, S. Iqbal, T. Hussain, W.L. Cheung, S. Ahmad Khan et al., Zn–Co-MOF on solution-free CuO nanowires for flexible hybrid energy storage devices. Mater. Today Phys. **23**, 100655 (2022). https://doi.org/10.1016/j.mtphys.2022.100655
86. I. Hussain, S. Iqbal, T. Hussain, Y. Chen, M. Ahmad et al., An oriented Ni–Co-MOF anchored on solution-free 1D CuO: a p–n heterojunction for supercapacitive energy storage. J. Mater. Chem. A **9**, 17790–17800 (2021). https://doi.org/10.1039/D1TA04855D
87. I. Hussain, T. Hussain, M. Ahmad, X. Ma, M.S. Javed et al., Modified KBBF-like material for energy storage applications: $ZnNiBO_3(OH)$ with enhanced cycle life. ACS Appl. Mater. Interfaces **14**, 8025–8035 (2022). https://doi.org/10.1021/acsami.1c23583
88. I. Shaheen, I. Ali, F. Bibi, A. Hanan, M. Ahmad et al., Integrating 1d/2d nanostructure based on ni–co-oxalate for energy storage applications. Ceramics Int. **50**, 10789–10796 (2024). https://doi.org/10.1016/j.ceramint.2023.12.394
89. H. Shao, K. Xu, Y.-C. Wu, A. Iadecola, L. Liu et al., Unraveling the charge storage mechanism of $Ti_3C_2T_x$ MXene electrode in acidic electrolyte. ACS Energy Lett. **5**, 2873–2880 (2020). https://doi.org/10.1021/acsenergylett.0c01290
90. J. Yan, C.E. Ren, K. Maleski, C.B. Hatter, B. Anasori et al., Flexible MXene/graphene films for ultrafast supercapacitors with outstanding volumetric capacitance. Adv. Funct. Mater. **27**, 1701264 (2017). https://doi.org/10.1002/adfm.201701264
91. Q. Yang, Z. Xu, B. Fang, T. Huang, S. Cai et al., MXene/graphene hybrid fibers for high performance flexible supercapacitors. J. Mater. Chem. A **5**, 22113–22119 (2017). https://doi.org/10.1039/c7ta07999k
92. C.J. Zhang, V. Nicolosi, Graphene and MXene-based transparent conductive electrodes and supercapacitors. Energy Storage Mater. **16**, 102–125 (2019). https://doi.org/10.1016/j.ensm.2018.05.003
93. X. Liu, F. Xu, Z. Li, Z. Liu, W. Yang et al., Design strategy for MXene and metal chalcogenides/oxides hybrids for supercapacitors, secondary batteries and electro/photocatalysis. Coord. Chem. Rev. **464**, 214544 (2022). https://doi.org/10.1016/j.ccr.2022.214544
94. Q. Jiang, N. Kurra, M. Alhabeb, Y. Gogotsi, H.N. Alshareef, All pseudocapacitive MXene-RuO_2 asymmetric supercapacitors. Adv. Energy Mater. **8**, 1703043 (2018). https://doi.org/10.1002/aenm.201703043
95. D. Wang, J. Si, S. Lin, R. Zhang, Y. Huang et al., Achieving macroscopic $V_4C_3T_x$ MXene by selectively etching Al from V_4AlC_3 single crystals. Inorg. Chem. **59**, 3239–3248 (2020). https://doi.org/10.1021/acs.inorgchem.9b03625
96. X. Bin, M. Sheng, Y. Luo, W. Que, Self-assembling delaminated $V_4C_3T_x$ MXene into highly stable pseudocapacitive flexible film electrode for supercapacitors. Adv. Mater. Interfaces **9**, 2200231 (2022). https://doi.org/10.1002/admi.202200231
97. S. Zhao, X. Meng, K. Zhu, F. Du, G. Chen et al., Li-ion uptake and increase in interlayer spacing of Nb_4C_3 MXene. Energy Storage Mater. **8**, 42–48 (2017). https://doi.org/10.1016/j.ensm.2017.03.012
98. S. Zhao, X. Wang, N. Kurra, Y. Gogotsi, Y. Gao, Effect of pinholes in Nb_4C_3 MXene sheets on its electrochemical behavior in aqueous electrolytes. Electrochem. Commun. **142**, 107380 (2022). https://doi.org/10.1016/j.elecom.2022.107380
99. Q. Peng, J. Rehman, K. Eid, A.S. Alofi, A. Laref et al., Vanadium carbide (V_4C_3) MXene as an efficient anode for Li-ion and Na-ion batteries. Nanomaterials **12**, 2825 (2022). https://doi.org/10.3390/nano12162825
100. P.A. Shinde, A.M. Patil, S. Lee, E. Jung, S. Chan Jun, Two-dimensional MXenes for electrochemical energy storage applications. J. Mater. Chem. A **10**, 1105–1149 (2022). https://doi.org/10.1039/d1ta04642j
101. C. Zhan, M. Naguib, M. Lukatskaya, P.R.C. Kent, Y. Gogotsi et al., Understanding the MXene pseudocapacitance. J. Phys. Chem. Lett. **9**, 1223–1228 (2018). https://doi.org/10.1021/acs.jpclett.8b00200
102. Y. Su, J. Shang, X. Liu, J. Li, Q. Pan et al., Constructing π-π superposition effect of tetralithium naphthalenetetracarboxylate with electron delocalization for robust dual-ion batteries. Angew. Chem. Int. Ed. (2024). https://doi.org/10.1002/anie.202403775
103. M. Zhang, W. Zhang, F. Zhang, C.-S. Lee, Y. Tang, Anion-hosting cathodes for current and late-stage dual-ion batteries. Sci. China Chem. (2024). https://doi.org/10.1007/s11426-023-1957-3
104. R. Akhter, S.S. Maktedar, MXenes: a comprehensive review of synthesis, properties, and progress in supercapacitor applications. J. Materiomics **9**, 1196–1241 (2023). https://doi.org/10.1016/j.jmat.2023.08.011
105. J. Huang, Z. Li, Y. Mao, Z. Li, Progress and biomedical applications of MXenes. Nano Sel. **2**, 1480–1508 (2021). https://doi.org/10.1002/nano.202000309
106. C. Ma, M.-G. Ma, C. Si, X.-X. Ji, P. Wan, Flexible MXene-based composites for wearable devices. Adv. Funct. Mater. **31**, 2009524 (2021). https://doi.org/10.1002/adfm.202009524
107. M.W. Barsoum, *Fundamentals of ceramics* (CRC Press, Boca Raton, 2019). https://doi.org/10.1201/9781498708166
108. Z. Wang, C. Wei, H. Jiang, Y. Zhang, K. Tian et al., MXene-based current collectors for advanced rechargeable batteries. Adv. Mater. **36**, e2306015 (2024). https://doi.org/10.1002/adma.202306015
109. X. Chen, S. Wang, J. Shi, X. Du, Q. Cheng et al., Direct laser etching free-standing MXene-MoS_2 film for highly flexible micro-supercapacitor. Adv. Mater. Interfaces **6**, 1901160 (2019). https://doi.org/10.1002/admi.201901160

 https://doi.org/10.1007/s40820-024-01418-0

110. X. Li, Y. Ma, Y. Yue, G. Li, C. Zhang et al., A flexible Zn-ion hybrid micro-supercapacitor based on MXene anode and V_2O_5 cathode with high capacitance. Chem. Eng. J. **428**, 130965 (2022). https://doi.org/10.1016/j.cej.2021.130965
111. B.C. Wyatt, A. Rosenkranz, B. Anasori, 2D MXenes: tunable mechanical and tribological properties. Adv. Mater. **33**, 2007973 (2021). https://doi.org/10.1002/adma.202007973
112. K.R.G. Lim, M. Shekhirev, B.C. Wyatt, B. Anasori, Y. Gogotsi et al., Fundamentals of MXene synthesis. Nat. Synth. **1**, 601–614 (2022). https://doi.org/10.1038/s44160-022-00104-6
113. C. Chen, X. Xie, B. Anasori, A. Sarycheva, T. Makaryan et al., MoS_2-on-MXene heterostructures as highly reversible anode materials for lithium-ion batteries. Angew. Chem. Int. Ed. **57**, 1846–1850 (2018). https://doi.org/10.1002/anie.201710616
114. S. Siddique, A. Waheed, M. Iftikhar, M.T. Mehran, M.Z. Zarif et al., Fluorine-free MXenes via molten salt lewis acidic etching: applications, challenges, and future outlook. Prog. Mater. Sci. (2023). https://doi.org/10.1016/j.pmatsci.2023.101183
115. L. Liu, H. Zschiesche, M. Antonietti, B. Daffos, N.V. Tarakina et al., Tuning the surface chemistry of MXene to improve energy storage: example of nitrification by salt melt. Adv. Energy Mater. **13**, 2202709 (2023). https://doi.org/10.1002/aenm.202202709
116. M. Wang, C. Jiang, S. Zhang, X. Song, Y. Tang et al., Reversible calcium alloying enables a practical room-temperature rechargeable calcium-ion battery with a high discharge voltage. Nat. Chem. **10**, 667–672 (2018). https://doi.org/10.1038/s41557-018-0045-4
117. X. Zhang, Y. Tang, F. Zhang, C.-S. Lee, A novel aluminum–graphite dual-ion battery. Adv. Energy Mater. **6**, 1502588 (2016). https://doi.org/10.1002/aenm.201502588
118. W. Lin, Y.-R. Lu, W. Peng, M. Luo, T.-S. Chan et al., Atomic bridging modulation of Ir–N, S Co-doped MXene for accelerating hydrogen evolution. J. Mater. Chem. A **10**, 9878–9885 (2022). https://doi.org/10.1039/d2ta00550f
119. K. Rajput, V. Kumar, S. Thomas, M.A. Zaeem, D.R. Roy, Ca_2C MXene monolayer as a superior anode for metal-ion batteries. 2D Mater. **8**, 035015 (2021). https://doi.org/10.1088/2053-1583/abf233
120. M. Hu, Z. Li, T. Hu, S. Zhu, C. Zhang et al., High-capacitance mechanism for $Ti_3C_2T_x$ MXene by in situ electrochemical Raman spectroscopy investigation. ACS Nano **10**, 11344–11350 (2016). https://doi.org/10.1021/acsnano.6b06597
121. C. Li, A.K. Tareen, K. Khan, J. Long, I. Hussain et al., Highly efficient, remarkable sensor activity and energy storage properties of MXenes and borophene nanomaterials. Prog. Solid State Chem. **70**, 100392 (2023). https://doi.org/10.1016/j.progsolidstchem.2023.100392
122. J. Jiang, S. Bai, J. Zou, S. Liu, J.-P. Hsu et al., Improving stability of MXenes. Nano Res. **15**, 6551–6567 (2022). https://doi.org/10.1007/s12274-022-4312-8
123. Y. Li, P. Kamdem, X.-J. Jin, In situ growth of chrysanthemum-like $NiCo_2S_4$ on MXenes for high-performance supercapacitors and a non-enzymatic H_2O_2 sensor. Dalton Trans. **49**, 7807–7819 (2020). https://doi.org/10.1039/d0dt01030h
124. M.R. Lukatskaya, O. Mashtalir, C.E. Ren, Y. Dall'Agnese, P. Rozier et al., Cation intercalation and high volumetric capacitance of two-dimensional titanium carbide. Science **341**, 1502–1505 (2013). https://doi.org/10.1126/science.1241488
125. R. Syamsai, A.N. Grace, G.A. Babu, K.B. Karuppanan, S.K. Eswaran et al., Titanium–tantalum double-ordered MXene nanosheets as supercapacitor electrodes. ACS Appl. Nano Mater. **6**, 5224–5232 (2023). https://doi.org/10.1021/acsanm.2c05081
126. D. Maldonado-Lopez, J.R. Rodriguez, V.G. Pol, R. Syamsai, N.G. Andrews et al., Atomic-scale understanding of Li storage processes in the Ti_4C_3 and chemically ordered $Ti_2Ta_2C_3$ MXenes: a theoretical and experimental assessment. ACS Appl. Energy Mater. **5**, 1801–1809 (2022). https://doi.org/10.1021/acsaem.1c03239
127. A. Rafieerad, A. Amiri, G.L. Sequiera, W. Yan, Y. Chen et al., Development of fluorine-free tantalum carbide MXene hybrid structure as a biocompatible material for supercapacitor electrodes. Adv. Funct. Mater. **31**, 2100015 (2021). https://doi.org/10.1002/adfm.202100015
128. S. Zhao, C. Chen, X. Zhao, X. Chu, F. Du et al., Flexible $Nb_4C_3T_x$ film with large interlayer spacing for high-performance supercapacitors. Adv. Funct. Mater. **30**, 2000815 (2020). https://doi.org/10.1002/adfm.202000815
129. M. Saraf, B. Chacon, S. Ippolito, R.W. Lord, M. Anayee et al., Enhancing charge storage of $Mo_2Ti_2C_3$ MXene by partial oxidation. Adv. Funct. Mater. **34**, 2306815 (2024). https://doi.org/10.1002/adfm.202306815
130. D. Gandla, F. Zhang, D.Q. Tan, Advantage of larger interlayer spacing of a $Mo_2Ti_2C_3$ MXene free-standing film electrode toward an excellent performance supercapacitor in a binary ionic liquid-organic electrolyte. ACS Omega **7**, 7190–7198 (2022). https://doi.org/10.1021/acsomega.1c06761
131. D. Pinto, B. Anasori, H. Avireddy, C.E. Shuck, K. Hantanasirisakul et al., Synthesis and electrochemical properties of 2D molybdenum vanadium carbides–solid solution MXenes. J. Mater. Chem. A **8**, 8957–8968 (2020). https://doi.org/10.1039/d0ta01798a
132. H. Wang, Y. Xue, X. Song, S. Lei, H. Yu et al., Solid solution reinforced $V_3CrC_3T_x$ MXene cathodes for zn-ion micro-supercapacitors with high areal energy density and superior flexibility. J. Mater. Chem. A **10**, 20953–20963 (2022). https://doi.org/10.1039/D2TA04747K
133. Q. Wang, X. Zhang, Z. Chen, Y. Zhao, W. Yao et al., $Ti_{3-y}Nb_YC_2T_x$ MXenes as high-rate and ultra-stable electrode materials for supercapacitors. J. Alloys Compds. **954**, 170128 (2023). https://doi.org/10.1016/j.jallcom.2023.170128
134. R. Syamsai, A.N. Grace, Synthesis, properties and performance evaluation of vanadium carbide MXene as supercapacitor electrodes. Ceram. Int. **46**, 5323–5330 (2020). https://doi.org/10.1016/j.ceramint.2019.10.283